SAN FRANCISCO ESTUARY & WATERSHED SCIENCE
Published by the California Bay-Delta Authority Science Program and the John Muir Institute of the Environment

Low dissolved oxygen in an estuarine channel (San Joaquin River, California): mechanisms and models based on long-term time series

Alan D. Jassby
Department of Environmental Science and Policy, University of California at Davis
adjassby@ucdavis.edu

Erwin E. Van Nieuwenhuyse
Division of Environmental Affairs, U.S. Bureau of Reclamation

ABSTRACT

The Stockton Deep Water Ship Channel, a stretch of the tidal San Joaquin River, is frequently subject to low dissolved oxygen conditions and annually violates regional water quality objectives. Underlying mechanisms are examined here using the long-term water quality data, and the efficacy of possible solutions using time-series regression models. Hypoxia is most common during June-September, immediately downstream of where the river enters the Ship Channel. At the annual scale, ammonium loading from the Regional Wastewater Control Facility has the largest identifiable effect on year-to-year variability. The longer-term upward trend in ammonium loads, which have been increasing over 10% per year, also corresponds to a longer-term downward trend in dissolved oxygen during summer. At the monthly scale, river flow, loading of wastewater ammonium and river phytoplankton, Ship Channel temperature, and Ship Channel phytoplankton are all significant in determining hypoxia. Over the recent historical range (1983–2003), wastewater ammonium and river phytoplankton have played a similar role in the monthly variability of the dissolved oxygen deficit, but river discharge has the strongest effect. Model scenarios imply that control of either river phytoplankton or wastewater ammonium load alone would be insufficient to eliminate hypoxia. Both must be strongly reduced, or reduction of one must be combined with increases in net discharge to the Ship Channel. Model scenarios imply that preventing discharge down Old River with a barrier markedly reduces hypoxia in the Ship Channel. With the Old River barrier in place, unimpaired or full natural flow at Vernalis would have led to about the same frequency of hypoxia that has occurred with actual flows since the early 1980s.

KEYWORDS

Ammonium, dissolved oxygen, estuary, flow, hypoxia, time series model, phytoplankton, river, wastewater, water quality

INTRODUCTION

The lower San Joaquin River, one of two major rivers draining into the San Francisco Estuary, is frequently subject to low dissolved oxygen conditions and annually violates regional water quality objectives. The violations usually occur between June and November over a 20-km river reach immediately downstream of the city of Stockton. This reach is part of the Stockton Deep Water Ship Channel, a portion of the river between San Francisco Bay and the city that has been dredged to allow the passage of ocean-going vessels to the city's port. Dissolved oxygen concentrations can be chronically below regional water quality objectives and reach below 2.5 mg L^{-1} at times. These low oxygen conditions interfere with several beneficial uses of the river, including spawning and migration of both warm (striped bass, sturgeon, and shad) and cold (salmon and steelhead) freshwater fishes, as well as warm and cold freshwater species habitat (CVRWQCB 2003). For example, oxygen depletion is believed to act as a barrier to migration of fall-run Chinook salmon (*Oncorhynchus tshawytscha*) upriver between September and December to spawn in the Merced, Tuolumne, and Stanislaus rivers (Hallock and others 1970). Moreover, low dissolved oxygen has recently been severe enough to kill both steelhead and salmon, as reported in *The Record* (Stockton), 8 July 2003.

Under Section 303(d) of the 1972 federal Clean Water Act, states are required to develop a list of waters that do not meet water quality standards, even after installation of minimum required levels of pollution control technology, and to develop an action plan to improve water quality. The Central Valley Regional Water Quality Control Board (Regional Board) adopted a revised 303(d) list that identified low dissolved oxygen levels in the lower San Joaquin River as a high priority problem, thereby committing to determining the assimilative capacity of the impaired river reach (Total Maximum Daily Load, or TMDL) and to allocating responsibility for the waste load among possible sources (CVRWQCB 2003). Under the auspices of the Regional Board, a group of interested parties or stakeholders organized the San Joaquin River Dissolved Oxygen TMDL Steering Committee, which initiated a series of field, laboratory, and modeling studies funded by the California Bay-Delta Authority and other sources.

These ongoing studies have yielded insights into the mechanisms underlying hypoxia in the river and the role of different organic matter sources and other contributory factors (Lee and Jones-Lee 2002). As a whole, they also confirm early research that identified the main factors affecting hypoxia in the Ship Channel (Bain and others 1968). According to these studies, there are two main sources of oxygen-demanding materials: the Stockton Regional Wastewater Control Facility (Wastewater Facility), which discharges into the San Joaquin River just upstream of the Ship Channel, and materials from nonpoint sources further upstream. The actual effect of these materials on Ship Channel dissolved oxygen depends on three main factors: morphometry of the Ship Channel, which affects the impact of natural aeration mechanisms and of oxygen-demanding reactions on dissolved oxygen concentrations; flow rate through the Ship Channel, which affects loading rates of oxygen-demanding materials and dissolved oxygen, as well as the residence time during which potential oxygen demand is actually realized in the Ship Channel; and environmental factors such as temperature. Because of gaps and uncertainties in current understanding, however, the TMDL is phased to allow for further technical studies of the relative roles of different oxygen-demanding substances and

their interactions with Ship Channel morphometry and flow.

One relevant resource that has not been used extensively in this research effort is the large collection of retrospective data for the upper estuary. Several government agencies have maintained monitoring programs for decades, mostly for determining compliance with water quality objectives. Recently, we used these data to investigate regulation of phytoplankton concentrations in the tidal San Joaquin River upstream of the Ship Channel (Jassby 2005). Our purpose here is to determine what this extensive historical monitoring dataset going back to the 1960s can tell us about the nature of hypoxia in the Ship Channel and the mechanisms underlying it. The scope is limited in that we confine ourselves to the ramifications of the monitoring dataset rather than attempt to include the large amount of current and recent field research on the issue. The historical dataset allows us to examine hypotheses developed from a few years of study in a much longer context. Observations over shorter time scales, in which a causative factor remains relatively constant, can lead to distorted views about the long-term importance of underlying mechanisms. The interannual variability in runoff to the Delta varies by an order of magnitude, which is sure to change the relative importance of different mechanisms in different years. The nature of the historical data, in the end, dictates the specific issues that can be addressed and the approaches that are feasible. Specifically, the data allowed us to undertake the following analyses: First, the spatial and temporal patterns of hypoxia are summarized from a long-term perspective. We then examine the statistical evidence for the relative importance of different causal factors. Finally, we use a time-series model to examine how the historical patterns might have been different under different management scenarios.

Study Area

The tidal San Joaquin River is located in the upper part of the estuary known as the Sacramento-San Joaquin Delta (Delta), a mosaic of waterways linking the rivers of northern California to the downstream embayments comprising San Francisco Bay (Bay); together, the Delta and Bay form the San Francisco Estuary. Delta inflows comprise, on average, 84% Sacramento River flow, 13% San Joaquin River flow, and 3% from smaller rivers. The San Joaquin River extends from the Delta upstream past the city of Fresno, draining a watershed area of about 19,000 km^2 (Figure 1 in Jassby 2005). Its river valley is a major center of agricultural production. Despite the loss of most of its wetlands, the watershed also remains a critical habitat for fish and wildlife, including many federally listed threatened and endangered plants and animals. Hydrology of the river and its major tributaries—the Merced, Tuolumne, and Stanislaus rivers—upstream of the Delta is highly managed through dams, diversions, and artificial conveyances. The river reaches the southern boundary of the Delta near the town of Vernalis, where estuarine tides begin to affect its flow (Figure 1). The long-term (1956–2002) mean flow at this point is about 130 $m^3 s^{-1}$, with annual means ranging from 13 $m^3 s^{-1}$ in 1961 to 650 $m^3 s^{-1}$ in 1983 (IEP 2003). For comparison, the unimpaired or full natural flow for the period 1951–2000 was about 240 $m^3 s^{-1}$, of which about 72 $m^3 s^{-1}$ was provided by the mainstem above the major tributaries (CDWR 2004a). The construction of Friant Dam and formation of Millerton Lake in the 1940s, and subsequent diversion of these mainstem waters for irrigation, has led to a dewatering of about 100 km of the river. Past Mossdale, a portion of the water is diverted down Old River to Clifton Court Forebay, where it is exported for agricultural, industrial, and domestic use, including drinking water for 22 million state residents, through large pumping facilities feeding the State Water

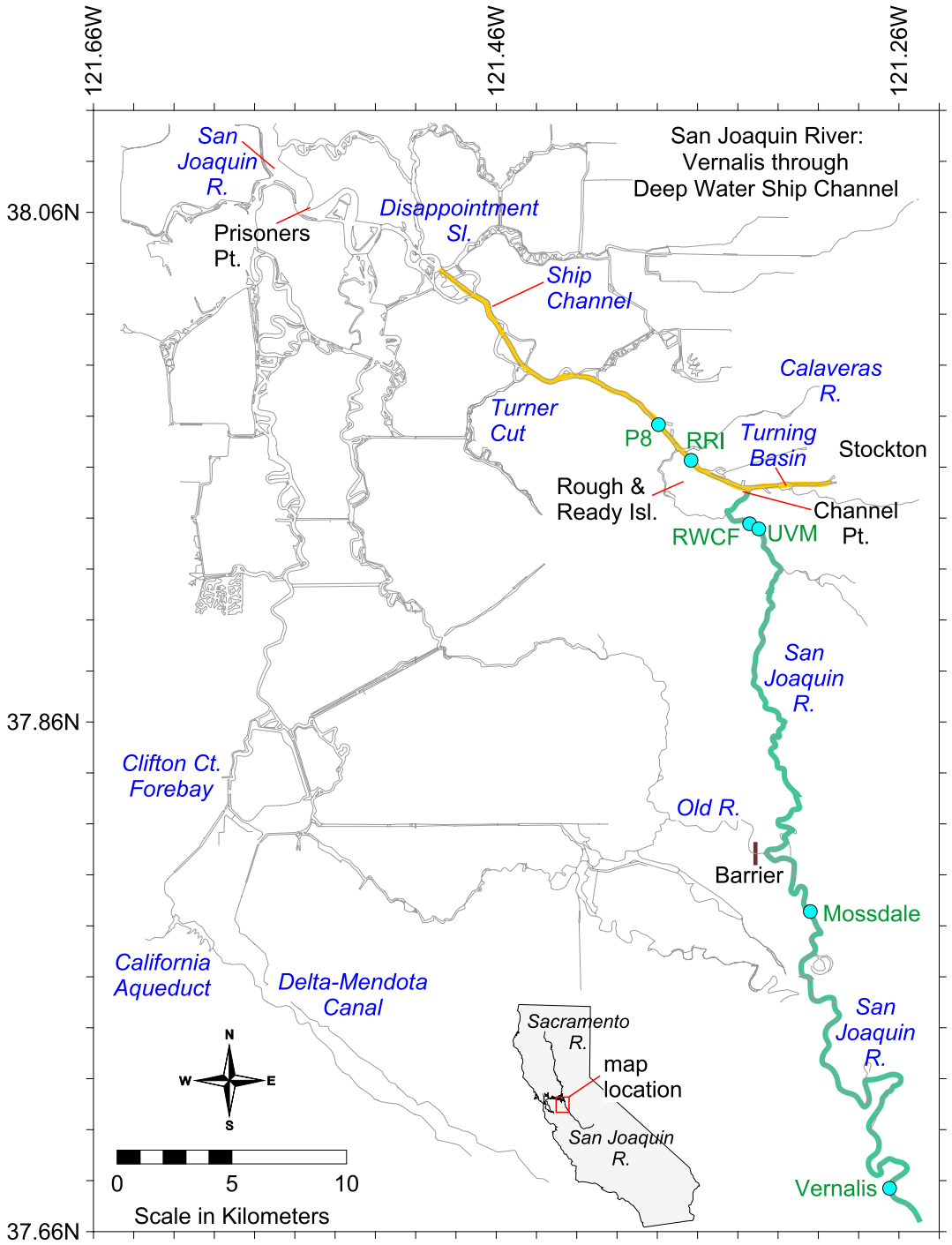

Figure 1. The San Joaquin River from Vernalis through the Stockton Deep Water Ship Channel. The locations of the Vernalis, Mossdale, and Buckley Cove (P8) long-term monitoring stations are indicated, as well as the tidal velocity station that utilizes an Ultrasonic Velocity Meter (UVM), Regional Wastewater Control Facility discharge point (RWCF), and Stockton continuous monitoring station at Rough and Ready Island (RRI). Green line, tidal portion of the river upstream of the Ship Channel. Yellow line, dissolved oxygen-impaired portion of the Ship Channel.

Project (California Aqueduct) and federal Central Valley Project (Delta-Mendota Canal). Annually, temporary barriers have been placed at the head of Old River to increase flows down the mainstem, with the intention of alleviating low dissolved oxygen conditions downstream and facilitating fish migration. Water is also diverted for irrigation in the Delta by numerous siphons; much of this water is lost to evapotranspiration, although some returns through many agricultural drainage points. The river is about 2 to 4 m deep and 50 m wide between Vernalis station and the Ship Channel. Just upstream of the Ship Channel, the Wastewater Facility discharges its effluent into the river. The river enters the Ship Channel at Channel Point. River width increases to about 75 m in the Ship Channel, and it is dredged to a depth of 11 m between the Port of Stockton and the Bay (Figure 2). The tidal range is about 1 m in this region. Low dissolved oxygen conditions occur in the Ship Channel from approximately the Turning Basin at the Port of Stockton downstream to Turner Cut, sometimes extending to Disappointment Slough.

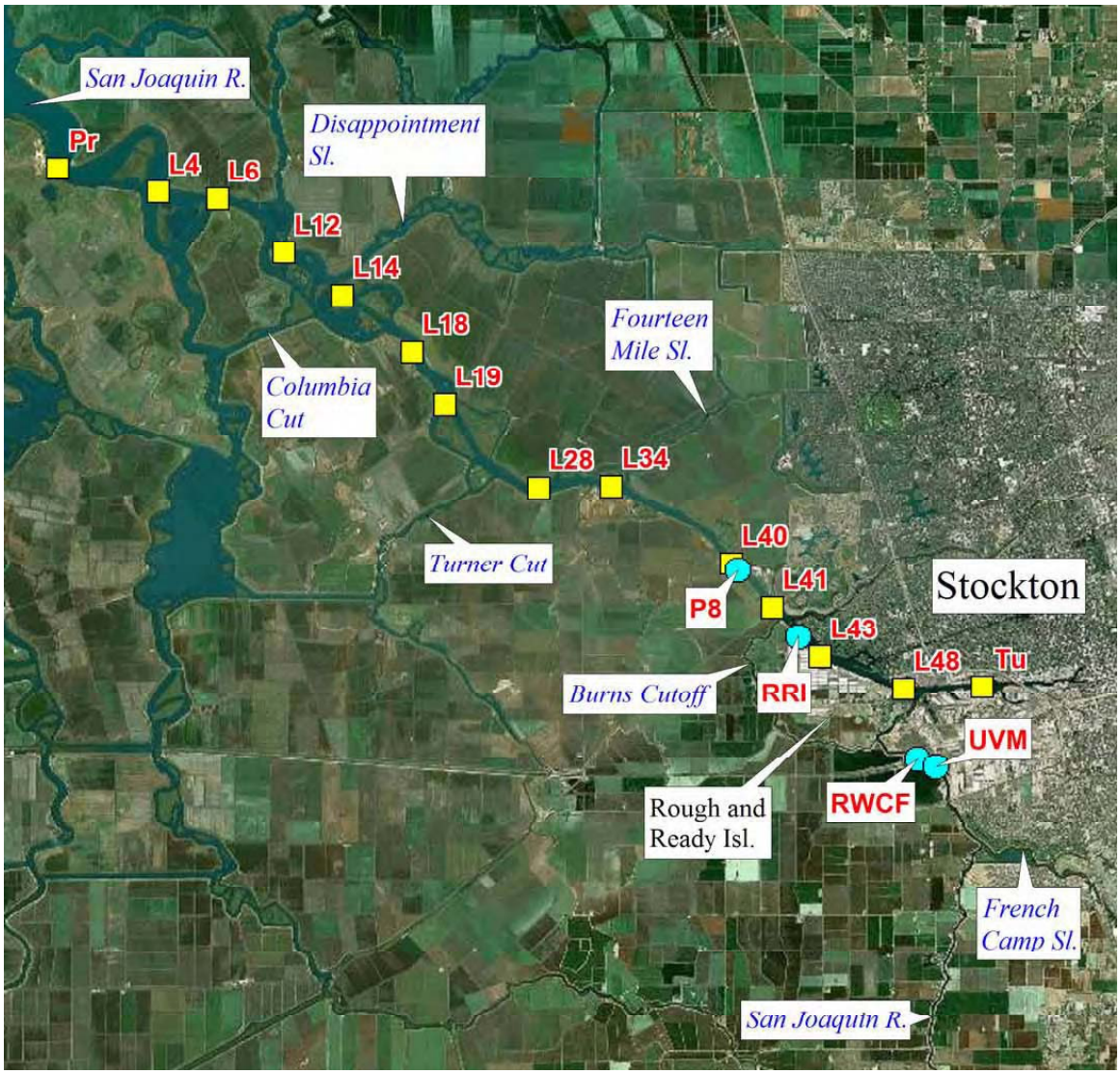

Figure 2. Satellite photograph of the water quality-impaired portion of the Ship Channel. Abbreviations are the same as in Figure 1 and Table 2.

METHODS

Data Sources

A variety of data sources were used in this study, some of them extending back to the 1960s (Table 1). The frequencies shown are approximate, and some datasets have large gaps in them. Relevant stations are indicated on the maps (Figure 1 and Figure 2).

A California Department of Water Resources monitoring program measures surface and bottom dissolved oxygen at 14 stations in the San Joaquin River, from Prisoners Point to the Stockton Turning Basin, biweekly to monthly during July–December (Table 2). These data are useful for showing the spatial and seasonal extent of hypoxia over the years, although they are not sufficient for detailed analysis of mechanisms.

The discrete water quality monitoring program collects data from throughout the Delta on a monthly basis, approximately. The program was originally started by the U.S. Bureau of Reclamation in the late 1960s. It is now carried out jointly with the California Department of Water Resources, assisted by the California Department of Fish and Game and the U.S. Geological Survey, under the auspices of the Interagency Ecological Program's Environmental Monitoring Program.

Its primary purpose is to provide information for compliance with flow-related water quality standards specified in water rights permits that allow export by the state and federal water projects. The stations relevant to this study are the Vernalis and Mossdale stations on the tidal river upstream of the Ship Channel, and Buckley Cove station in the Ship Channel itself (Figure 1 and Figure 2). Water quality variables reported here include mainly chlorophyll *a* and temperature. A detailed description of the sampling and analytical methods can be accessed at http://www.iep.ca.gov/emp/Metadata/metadata_index.html.

The continuous water quality monitoring program collects data from seven fixed sampling stations throughout the Delta, averaging and recording on an hourly basis. This effort is also part of the Environmental Monitoring Program. The data are used to track environmental conditions in the Delta and Suisun Bay, for operation of the State Water Project and Central Valley Project, and as input to hydrodynamic and water quality models. Water is collected from about one meter below the surface. The only time series from the program used here are the dissolved oxygen data from the Stockton station at Rough and Ready Island near Burns Cutoff (Figure 1).

Daily ammonium loads from the Wastewater Facility were calculated as follows: If the record had entries for effluent discharge and ammonium concentration, they were simply multiplied together. If the record had entries for discharge but not concentration, the daily load was estimated using the flow-weighted mean concentration for the month. If there was no record for discharge, then the load was assumed to be zero for that day. Monthly averages were then estimated by the arithmetic mean of daily loads. The proportion of BOD due to ammonium in Wastewater Facility effluent was estimated by $4.57N_{amm}/(4.57N_{amm} + 4.57N_{org} + 2.5C_{bod5})$, where N_{amm} is ammonium nitrogen, N_{org} is organic nitrogen, and C_{bod5} is the five-day carbonaceous BOD. The conversion of ammonium to nitrate is assumed to require 4.57 g O (g N)$^{-1}$ (Chapra 1997). The factor of 2.5 for converting five-day to ultimate carbonaceous BOD was used in accordance with previous analyses of dissolved oxygen in the Ship Channel (Lee and Jones-Lee 2002).

Table 1. Data sources.

Program	*Agency*	*Frequency*
Dissolved oxygen	Calif. Dept. of Water Resources	biweekly, Aug.–Nov.
Discrete water quality	Interagency Ecological Program	monthly
Continuous water quality	Interagency Ecological Program	hourly
Wastewater Facility effluent	City of Stockton	daily
Dayflow	Interagency Ecological Program	daily
Tidal velocity	U.S. Geological Survey	15-minute

Table 2. Long-term stations for characterizing hypoxia in the Ship Channel with biweekly surface and bottom measurements.

Name	*Label*	*Longitude*	*Latitude*
Prisoners Pt.	Pr	–121.557	38.060
Light 4	L4	–121.531	38.055
Light 6	L6	–121.516	38.054
Light 12	L12	–121.499	38.043
Light 14	L14	–121.484	38.034
Light 18	L18	–121.466	38.022
Light 19	L19	–121.457	38.011
Light 28	L28	–121.433	37.994
Light 34	L34	–121.414	37.994
Light 40	L40	–121.382	37.978
Light 41	L41	–121.372	37.969
Light 43	L43	–121.359	37.959
Light 48	L48	–121.338	37.952
Turning Basin	Tu	–121.318	37.952

The best estimate of historical mean daily flows in the Delta is obtained with Dayflow, a computer program developed in 1978 as an accounting tool for determining historical Delta boundary hydrology (IEP 2003). San Joaquin River discharge is estimated at Vernalis. Net discharge into the Ship Channel is lower, primarily because of the flow split at Old River (Figure 1). Dayflow output itself does not contain estimates of net discharge into the Ship Channel, but the U.S. Geological Survey has operated an Ultrasonic Velocity Meter station in the San Joaquin River just upstream of the Ship Channel since August 1995 (http://sfbay.wr.usgs.gov/access/delta/tidalflow; Figure 1). A 15-minute interval tidal flow record is computed and converted to discharge using water-surface elevation, channel geometry survey data, and Acoustic Doppler Current Profiler measurements. The proportion of flow down Old River depends on water exports and the presence or absence of a temporary rock barrier—the Head of Old River barrier—constructed annually at the confluence of the Old and San Joaquin rivers to protect outmigrating juvenile salmon from the federal and state pumping plants. The monthly average of measured net discharge values can be predicted using river discharge at Vernalis, water exports, and the state of the barrier, allowing construction of a surrogate net discharge series (Q_{net}, $m^3\ s^{-1}$) for the entire period of interest (Jassby 2005).

Unimpaired runoff or full natural flow represents the natural water production of a river basin, unaltered by upstream diversions, storage, or by export or import of water to or from other watersheds. We estimated monthly unimpaired runoff at Vernalis from the sum of estimates for the Stanislaus, Tuolumne, Merced, and San Joaquin rivers. These flows are based on calculations done by project operators on the respective rivers, the U.S.

Army Corps of Engineers, and/or California Cooperative Snow Surveys (CDWR 2004a).

The monthly time series of photosynthetically active radiation (PAR) is based on daily irradiance for Davis, California, the nearest location for which a complete record is available (CDWR 2004b). A factor of 0.18 is used to convert daily mean irradiance (W m^{-2}) to PAR quantum irradiance (mol quanta m^2 d^{-1}), assuming PAR is 45% of total irradiance and a conversion of 2.77×10^{18} quanta s^{-1} W^{-1} for PAR (Morel and Smith 1974).

We used data reported by Lee and Jones-Lee (2002, Table D-3) to estimate the contribution of river phytoplankton to BOD. To convert chlorophyll *a* to organic carbon and then biochemical oxygen demand (BOD, mg L^{-1}) equivalents, the phytoplankton chlorophyll *a* to carbon ratio (Chl:C) is required. Cloern and others (1995) developed an empirical expression for this ratio dependent on temperature, mean water column irradiance, and nutrient concentration, which was used to estimate the organic carbon equivalent of phytoplankton chlorophyll *a*. The details are described by Jassby (2005). The carbonaceous BOD for a typical phytoplankton cell is 2.69 g O (g C)$^{-1}$, and the nitrogenous BOD due to nitrification is 0.804 g O (g C)$^{-1}$, an additional 30% (Chapra 1997). The equivalent BOD for phytoplankton is therefore 3.49*B*/(Chl:C), where *B* (mg L^{-1}) represents chlorophyll *a* concentration.

Data Analysis and Modeling

Unless otherwise stated, replicate samples for all variables have been averaged and data within the same month aggregated by their median, in order to avoid bias when comparing seasons with different amounts of raw data. When necessary, small gaps in monthly time series were imputed using a time series modeling procedure known as TRAMO, an acronym for Time series Regression with ARIMA (Autoregressive Integrated Moving Average) noise, Missing observations, and Outliers (Gómez and Maravall 2002). Appropriately, “tramo” is also a Spanish word meaning section or segment. TRAMO is an algorithm for estimation and forecasting of regression models with possibly nonstationary (ARIMA) errors and missing values. It is widely used in the European Union for modeling and forecasting economic time series. The program interpolates missing values based on the autocorrelation structure in the series, and optionally identifies and corrects for several types of outliers as well as intervention variable effects. We used the procedure for interpolating missing values with automatically selected ARIMA models and without outlier correction.

Multivariate models were estimated first using ordinary least squares. The distribution and correlogram of residuals were examined, and an autoregressive model for the residuals was then proposed. The equation for the residuals was substituted into the multivariate model, which was then solved by applying a Marquardt nonlinear least-squares algorithm. To guard against the presence of any further autocorrelation or heteroskedasticity, the standard errors were estimated conservatively using the Newey-West estimator (Newey and West 1987). The presence of any remaining serial and higher-order residual autocorrelation was tested using the Ljung-Box Q-statistics and the Breusch-Godfrey Lagrange multiplier test (Harvey 1993).

Simultaneous-equation models were solved with the Gauss-Seidel algorithm in dynamic mode to establish a baseline condition and to explore scenarios. In a dynamic solution, only values of the response variable from before the solution time period are used when determining the forecast. Subsequent values of lagged variables are

calculated from solutions for previous periods, not from actual historical values. This is the correct method for evaluating how a multi-step forecast would have performed historically, as opposed to the fitted solution, which is essentially a "one-step-ahead" forecast. The baseline solution in which no predictor series were altered was compared with various scenarios in which one or more predictors were changed. Scenarios were compared in terms of the empirical cumulative distribution function for the monthly dissolved oxygen deficit, defined as the (positive) difference between the monthly mean of minimum daily dissolved oxygen and a goal of 5 mg L^{-1}. Also, the proportion of months in which a positive deficit occurred was used as a scalar index for each scenario.

RESULTS

Hypoxia Patterns

First we summarize the spatial and temporal extent of hypoxia in the Ship Channel, insofar as the available data permit and with respect to the Regional Board's dissolved oxygen goals. The proposed interim performance goal is to prevent dissolved oxygen concentrations from falling below 5.0 mg L^{-1}, measured as a seven-day mean of daily minima, with no daily minimum below 3.0 mg L^{-1} (Gowdy and Foe 2002). The goal would be applicable at all locations within the Ship Channel between Channel Point and Disappointment Slough during June–November. At other times of the year, the Basin Plan objective of 5.0 mg L^{-1} minimum (CVRWQCB 1998) would be applicable. There is an additional existing Basin Plan objective of 6.0 mg L^{-1} minimum between Turner Cut and Stockton during September–November.

We made a composite of the discrete dissolved oxygen data by calculating the frequency of hypoxia (defined for this purpose as bottom dissolved oxygen <5.0 mg L^{-1}) for each of the months and years in which all stations were sampled (August–October of 1987, 1989, and 1991-2002; Figure 3). Hypoxia in the San Joaquin River (not including the Turning Basin) is most frequent from Lights 40 through 43 in August and September; it occurred at this time and region 60% to 80% of the time in the existing historical record. Hypoxia generally decreases in October at these stations, but can increase further downstream at Lights 19 and 28. The Turning Basin exhibits the most intense hypoxia, whereas hypoxia frequency at the most upstream Ship Channel station, Light 48, is actually less than in both the Basin and stations immediately downstream.

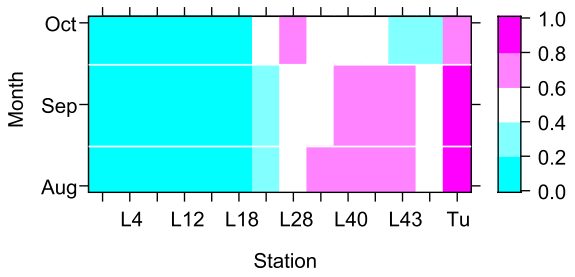

Figure 3. Proportion of observations for which bottom dissolved oxygen < 5 mg L^{-1} in the Ship Channel for each of August, September, and October. Proportions are based on data for 1987, 1989, 1991-2002.

We also plotted the data for each year with existing dissolved oxygen objectives in mind, to illustrate the scope of the existing problem (Figure 4). Interannual variability is high. The effect of climate is apparent. Consider the period 1991-present, during which data collection was relatively complete. The low precipitation of 1991 and 1992 coincided with unusually low dissolved oxygen in the Ship Channel that same summer and autumn. Similarly, the high precipitation of 1998 was accompanied by higher than usual dissolved oxygen. Climate is not an infallible guide to the patterns, however, especially as net discharge

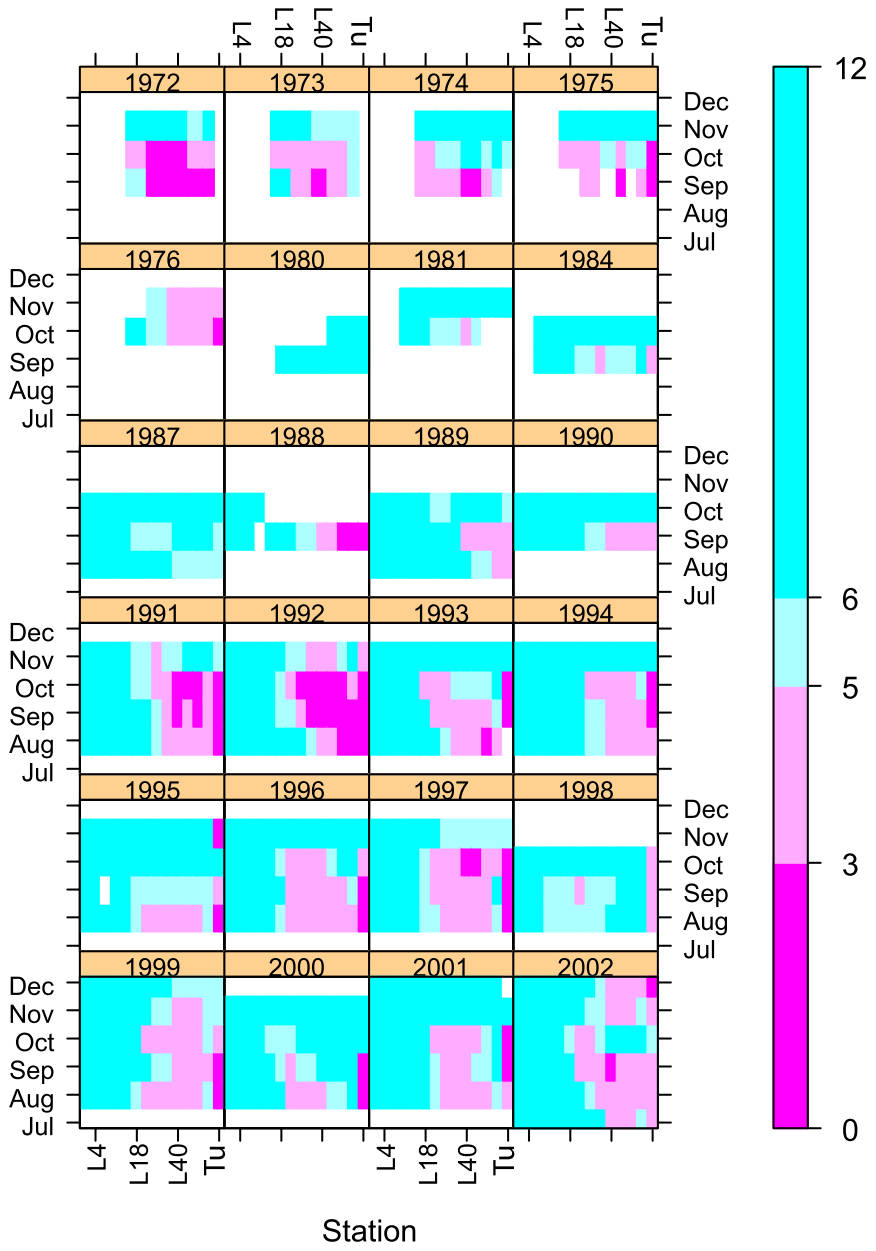

Figure 4. Spatial and seasonal patterns of bottom dissolved oxygen (mg L^{-1}) in the Ship Channel for individual years, based on data from 14 stations (see Table 2 for station descriptions).

into the Ship Channel depends not only on precipitation, but also on reservoir storage-and-release patterns and water exports down Old River. Unfortunately, the relatively low sampling frequency and the varying diel sampling time imply a high uncertainty in the actual monthly dissolved oxygen distributions.

The data are also useful for examining the relationship between surface (i.e., 1 m depth) and bottom dissolved oxygen. This relationship is important for understanding the relevance of the continuous dissolved oxygen monitoring data, which represent water collected from a single depth at 1 m. (The intake is enclosed and protected by a vertical perforated pipe

extending from 1 to 5 m, approximately, so the sample actually integrates 4 m of the water column.) We focus on stations L40, L41, and L43, which encompass the location of the continuous sensor and are also the locations of most intense hypoxia. Generally speaking, there is a strong correlation between surface and bottom dissolved oxygen (Figure 5). The relationship is weaker, however, earlier in the season. Increased phytoplankton productivity in surface waters and greater susceptibility to thermal stratification promotes the largest vertical differences in summer. In fact, there is at best a weak correlation between the two in August when bottom dissolved oxygen <5 mg L^{-1}. This means that high surface dissolved oxygen does not always imply high bottom dissolved oxygen. On the other hand, surface dissolved oxygen below 5 mg L^{-1} almost always ensures low bottom dissolved oxygen (Figure 6). Although 7 mg L^{-1} surface dissolved oxygen, for example, ensures that bottom dissolved oxygen is less than 5 mg L^{-1} only about 60% of the time, 5 mg L^{-1} surface dissolved oxygen ensures it more than 95% of the time. A surface dissolved oxygen value less than 5 mg L^{-1} is, accordingly, a conservative indication of bottom hypoxia.

Despite the availability of only near-surface dissolved oxygen conditions for most of the historical record, data from the continuous water quality monitoring station at Rough and Ready Island are informative about the temporal extent of hypoxia. These data include summaries of the hourly minimum dissolved oxygen for 1983–2003, from which we determined the daily minimum dissolved oxygen (Figure 7). Concentrations below 5 mg L^{-1} are quite common. Note also the severe hypoxia that occurred in February 2003. Although very low values were also recorded occasionally in other winters (1984, 1998, 1999), these previous observations were spikes and could have been artifacts, unlike the prolonged minimum in 2003. The methods used here are not suitable for understanding these infrequent winter events and so the emphasis is on the summer–autumn hypoxic conditions.

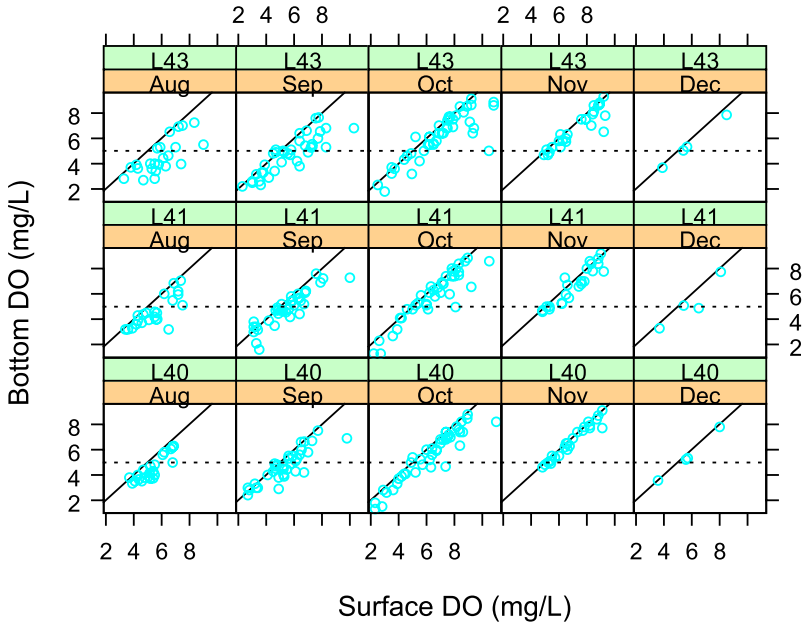

Figure 5. Bottom vs. surface dissolved oxygen in the Ship Channel, plotted by month and station. Solid line, 1:1 ratio. Dotted line, 5 mg L^{-1} bottom dissolved oxygen level.

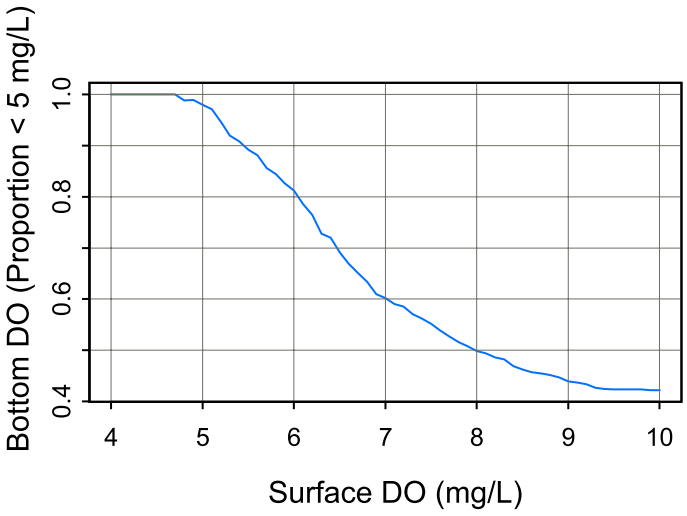

Figure 6. Proportion of bottom measurements < 5 mg L^{-1} for a given near-surface dissolved oxygen, based on biweekly data for Lights 40, 41, and 43.

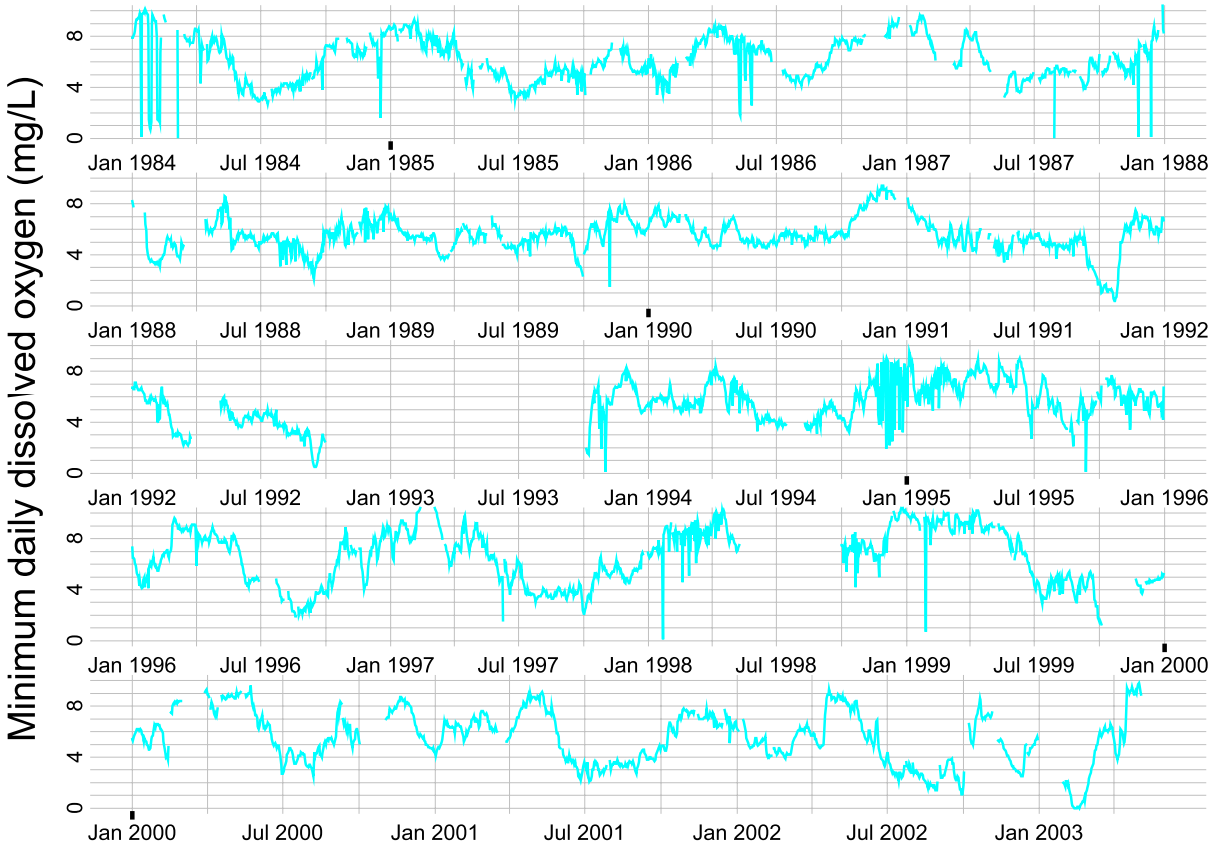

Figure 7. Daily minimum dissolved oxygen near the surface at the continuous monitoring station near Burns Cutoff.

The boxplots of Figure 8 summarize the seasonality of minimum dissolved oxygen for 1983–2002. The lowest values are typically observed during June–September, when even the long-term monthly medians are below 5 mg L^{-1}.

Variability at the Annual Scale

First we examine the relationship at the annual scale between mean daily minimum dissolved oxygen (O_{min}) and other variables thought to be important: net discharge (Q_{net}), river chlorophyll (B_{vern}), and Wastewater Facility ammonium load (L_{amm}). The use of B_{vern} as a surrogate for the long-term river BOD and L_{amm} as a surrogate for the long-term Wastewater Facility BOD load introduces additional uncertainty, but is necessitated by the absence of more complete long-term series for BOD sources (see "Discussion"). The number of years over which continuous dissolved oxygen has been measured is relatively small compared to the number of variables to be investigated, so it is vital to make maximum possible use of the data. River discharge at Vernalis, water exports, and the state of the Old River barrier are available for the entire period of interest, so a complete surrogate series for monthly Q_{net} can be constructed. The L_{amm} monthly series is also complete for the period 1983–2002. Gaps exist, however, for both O_{min} and B_{vern}, which were interpolated using the TRAMO procedure. The results are summarized in Figure 9A and 9B. The data gaps are small with regard to the series length, but interpolation significantly increases the number of years available for analysis.

It is most informative to create each annual series by averaging over the summer season, July–September, when hypoxia is typically at its worst (Figure 8). The data set available for analysis is limited by the dissolved oxygen series and extends only from 1984–2002, a total of 19 years. The four time series are plotted in Figure 10. Mean daily minimum dissolved oxygen is significantly correlated with Wastewater Facility ammonium loading and river phytoplankton chlorophyll *a*, but not net discharge, at the annual scale (Table 3). There are also correlations among the predictors, however, so that pairwise comparisons do not offer much distinction among potential causes.

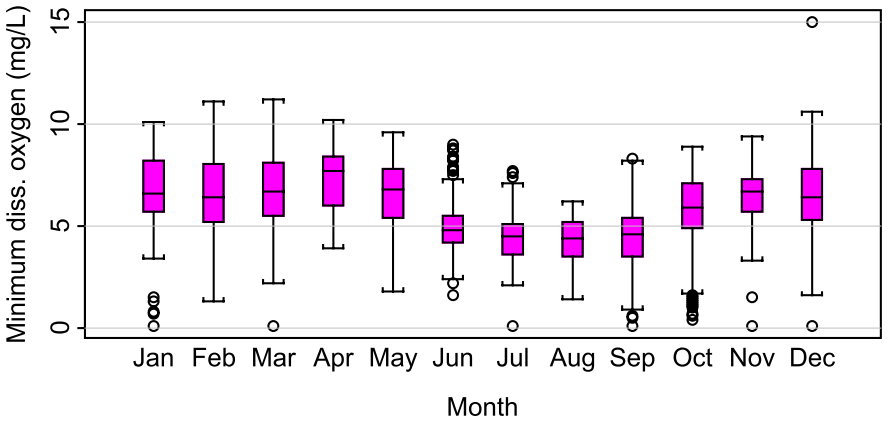

Figure 8. Monthly distributions of minimum dissolved oxygen based on 1983-2002 data from the continuous monitoring station near Burns Cutoff. Boxes extend from the first to third quartiles of the data, and the internal horizontal line marks the median. Vertical lines extending above and below each box encompass all data up to 1.5 interquartile distances (i.e., box heights) away from the median. Circles mark more extreme data values.

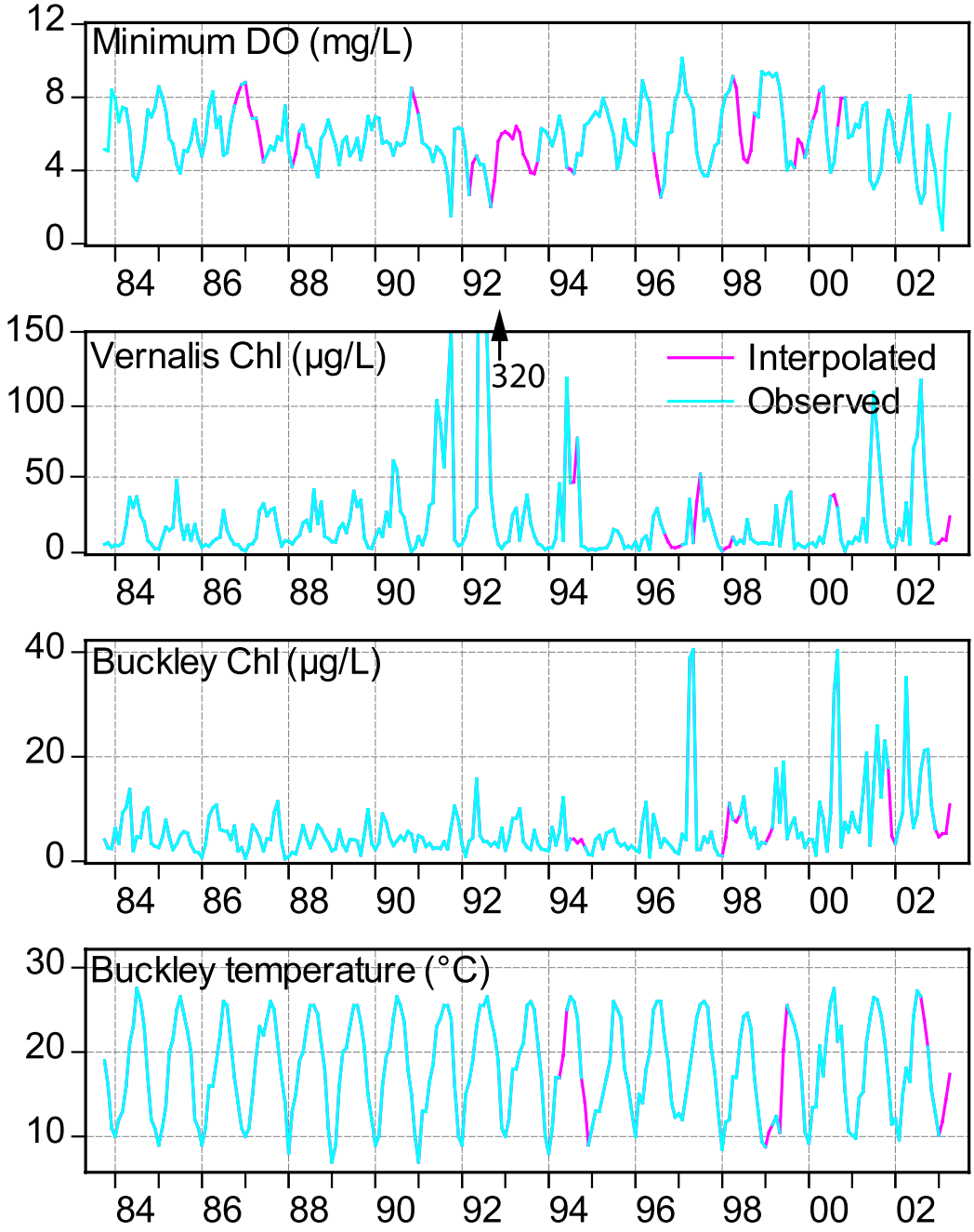

Figure 9. Monthly time series with interpolated data gaps for daily minimum dissolved oxygen in the Ship Channel; Vernalis chlorophyll *a* (note that the June 1992 value of 320 µg L^{-1} is off-scale); Buckley Cove chlorophyll *a*; and Buckley Cove temperature.

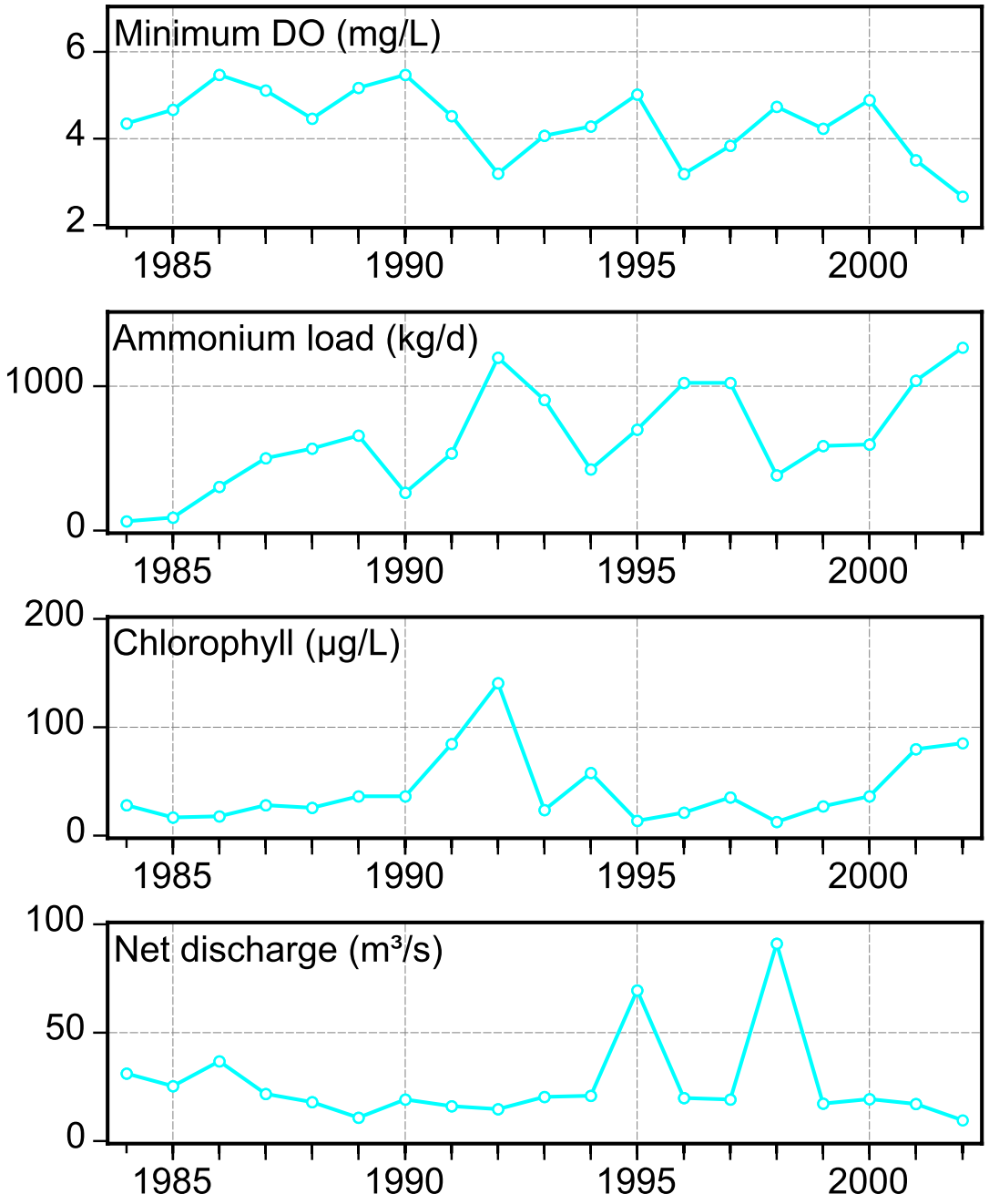

Figure 10. July-September averages for daily minimum dissolved oxygen at the continuous monitoring station in the Ship Channel; ammonium loading from the Wastewater Facility, chlorophyll *a* at Vernalis; and net river discharge into the Ship Channel.

Table 3. Correlations between minimum dissolved oxygen and predictor variables, interpolated and averaged over the summer, 1984–2002.

Variable	*r*	*P*
L_{amm}	–0.77	<0.001
B_{vern}	–0.57	0.011
Q_{net}	0.34	0.16

The relationship between dissolved oxygen and ammonium load is particularly striking for the period 1989–2002. Chlorophyll *a* concentrations in 1992 were exceptional, and that year should have provided a natural experiment to assess the effect of river phytoplankton, net discharge into the Ship Channel being approximately constant during 1990–1994; unfortunately, unusually high values of ammonium loading also occurred in 1992, complicating the interpretation of the low dissolved oxygen levels. The high chlorophyll *a* and ammonium concentrations were due largely to unusually low discharge rates upstream of the Delta.

Note also the long-term trend downward in summer dissolved oxygen (r = –0.53, P = 0.020) and upward in summer ammonium loading (r = 0.65, P = 0.003), in addition to the correspondence between their year-to-year fluctuations. (There is no serial correlation in the residuals about these trends to complicate the interpretation of the significance levels.) In fact, the lack of a year-to-year correspondence between the two prior to 1989 may have been simply because ammonium loading was too low relative to other factors in these earlier years. In contrast, neither river phytoplankton nor net discharge exhibit a long-term trend during summer. Summer ammonium loading increased several-fold during this period: the increase represented by the linear trend amounts to 370% from 1984 to 2002.

Variability at the Monthly Scale

We next examined variations in daily minimum dissolved oxygen at the monthly time scale. Monthly series for O_{min}, Q_{net}, B_{vern}, and L_{amm} were determined as above. One way to examine the potential role of flow, river phytoplankton, and wastewater effluent is to bin the dissolved oxygen data by different combinations of these three variables. The data for each variable were first divided into two classes, a low and a high one, separated by the median value, and a boxplot distribution was constructed for each combination of the resulting binary variables (Figure 11). The effect of any variable can be seen by comparing boxplot distributions in which the other two are held constant (data are not available for all possible comparisons). For example, the effect of river discharge at low and high ammonium loads can be seen by comparing A to B and C to D, respectively. River discharge has a strong positive effect on dissolved oxygen, regardless of ammonium load level. Similarly, comparing A to C and B to D demonstrates that high ammonium loading strongly depresses dissolved oxygen, whether river discharge is high or low. High chlorophyll also results in lower dissolved oxygen, at least at low river discharge (A versus E). Note, though, that when chlorophyll or ammonium load is already high, increasing the other one has no obvious additional effect (C or E versus G).

In further analyses, Ship Channel temperature (T_{chan}) and phytoplankton biomass as chlorophyll *a* (B_{chan}) were included as predictors using long-term monthly monitoring data from the station in Buckley Cove (P8, Figure 2). Temperature is a major factor in decomposition of organic matter, nitrification of ammonium, oxygen saturation, and other aspects of dissolved oxygen variability, and needs to be considered in any analysis involving seasonal changes. Phytoplankton affect the dissolved oxygen

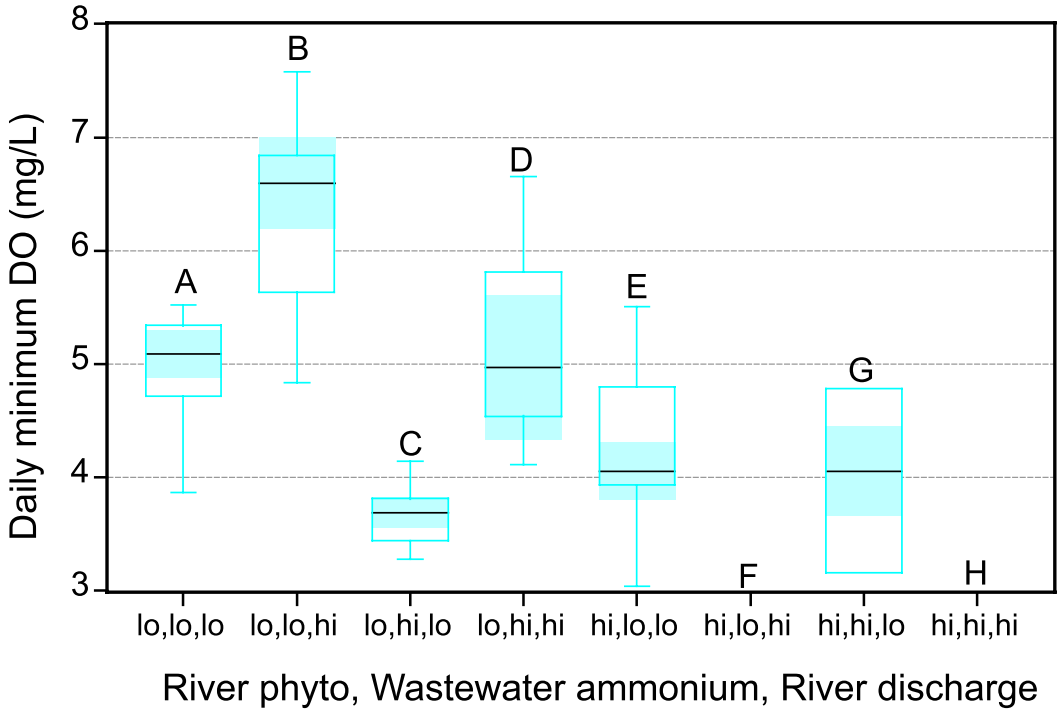

Figure 11. Distribution of the monthly means (July, August, September) of daily minimum dissolved oxygen, binned by various combinations of river chlorophyll *a*, Wastewater Facility ammonium load, and river discharge. lo, corresponding variable in x-axis title list is below its median; hi, corresponding variable in x-axis title list is above its median. Bin C (lo, hi, lo), for example, contains all oxygen values for which phytoplankton and discharge are below their respective median values and ammonium load is above its median value. Bins F and H contain no data because high phytoplankton and high discharge never occur simultaneously. Shaded areas represent 0.95 confidence intervals for the median.

balance through photosynthesis and respiration while alive, and decomposition after death. Missing data in temperature and chlorophyll *a* were imputed using the TRAMO algorithm (Figure 9C, 9D). The interpolation of missing data increases the available observations by more than 20% when all variables are used simultaneously, because the data gaps for different variables often do not coincide.

The importance of each of the five predictor variables—Q_{net} (m^3 s^{-1}), B_{vern} (µg L^{-1}), L_{amm} (kg d^{-1}), T_{chan} (°C), B_{chan} (µg L^{-1})—for the response variable O_{min} (mg L^{-1}) was explored using time series regression models. In particular, we viewed the dissolved oxygen variability as being linear in three processes: residence time in the Ship Channel as indexed by net discharge; decomposition of oxygen-demanding materials in the form of river phytoplankton and Wastewater Facility ammonium effluent; and phytoplankton metabolism in the Ship Channel itself as indexed by B_{chan}. To express river phytoplankton B_{vern} in terms of loading and therefore put it on a basis equivalent to L_{amm}, it must be multiplied by Q_{net}. The effect of both loading terms is highly dependent on reaction rates in the Ship Channel, which are controlled to a great extent by temperature. T_{chan} is accordingly included with the loading terms as

an interaction effect. Strongly skewed variables were log-transformed. The resulting equation is:

$$O_{min} = a_0 + a_1 \ln(Q_{net}) + [a_2 \ln(B_{vern}) \ln(Q_{net}) + a_3 L_{amm}] T_{chan} + a_4 \ln(B_{chan}) + \eta_t \quad \textbf{(1)}$$

where the a_i are constants and η_t is the unconditional residual at time *t*.

The multivariate linear model was estimated first using ordinary least squares and the residuals examined for autocorrelation. Autocorrelation was present, as would be expected when including variables with such strong seasonality. There may also be a physically-based persistence underlying the autocorrelation due to, for example, sedimentation of river phytoplankton and phytoplankton-derived detritus and prolonged decomposition in the Ship Channel. In any case, the standard assumptions of regression theory do not hold. The distribution and correlogram of residuals were examined, and an autoregressive model for the residuals was then proposed:

$$(1 - \rho_1 L - \rho_2 L^2) \eta_t = \varepsilon_t \quad \textbf{(2)}$$

where the ρ_i are constants and ε_t is normally distributed. *L* here represents the lag or backshift operator, i.e., $L^i x_t = x_{t-i}$. The resulting coefficient estimates are summarized in Table 4, and the fitted values are plotted in Figure 12. Note that missing data were not imputed in any of the series, so as not to influence patterns of autocorrelation.

All model parameters of this time-series regression model are statistically significant. The fitted values correspond well to observed ones $(R^2 = 0.73)$. All autocorrelations and partial autocorrelations are nearly zero at all lags. The Durbin-Watson statistic is 2.0, and *Q*-statistics are not significant up to at least 12 lags $P \geq 0.30$. In addition, the Breusch-Godfrey Lagrange multiplier test indicates no serial correlation up to at least 12 lags $(P = 0.32)$.

Table 4. Parameter estimates for model of daily minimum dissolved oxygen at the monthly scale. R^2 = 0.73, *n* = 208 after adjusting endpoints.

Term	*Coefficient*	*Std. Error*	*P*
Intercept	4.0	0.6	<0.001
$\ln(Q_{net})$	0.93	0.16	<0.001
$L_{amm} T_{chan}$	-3.6×10^{-5}	0.6×10^{-5}	<0.001
$\ln(B_{vern}) \ln(Q_{net}) T_{chan}$	-7.7×10^{-3}	1.1×10^{-3}	<0.001
$\ln(B_{chan})$	0.26	0.12	0.035
ρ_1	0.53	0.10	<0.001
ρ_2	–0.17	0.08	<0.036

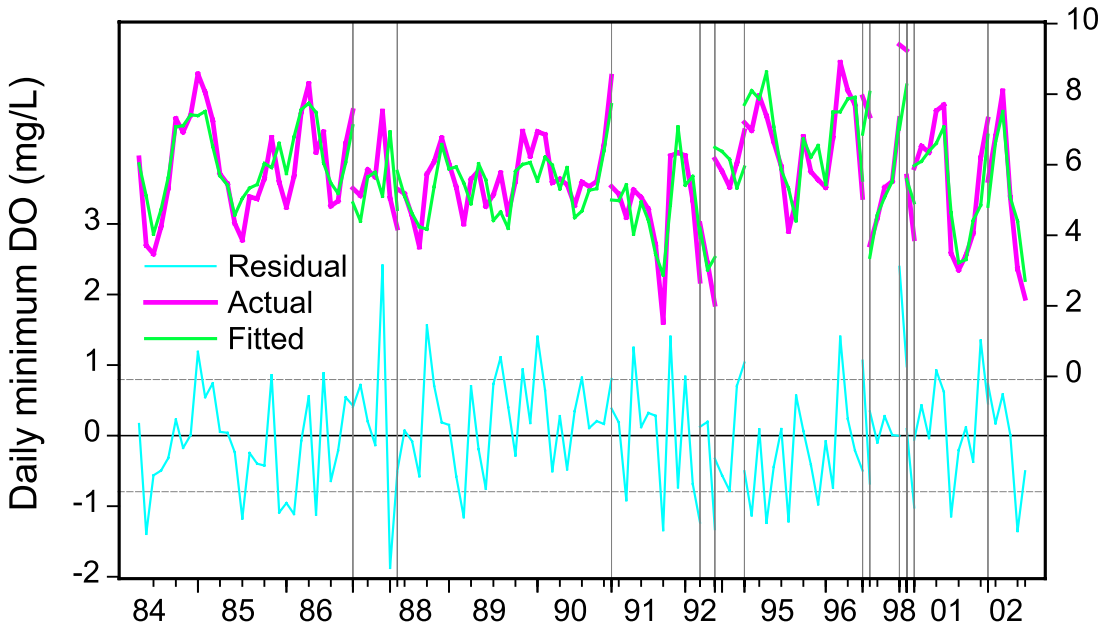

Figure 12. Observations compared with fitted values from the model of daily minimum dissolved oxygen in the Ship Channel (Equations 1 and 2). Vertical lines mark gaps in the monthly data for predictor or response variables.

Forecasting Scenarios

Next, the model was used in a forecasting mode in order to examine possible management strategies. In particular, changes in Wastewater Facility ammonium loading, upstream phytoplankton concentrations, and net discharge were explored. We assumed that ammonium loading could, in principle, be manipulated independently of the other predictor variables. We also assumed that reduction of nutrient loading could, in principle, be used to set a maximum attainable phytoplankton concentration independently of the other predictors. River flow, on the other hand, cannot be changed without corresponding changes in phytoplankton biomass, which is determined mostly by the time in transit from upstream to the Ship Channel. As a result, it is necessary to develop a coupled equation for B_{vern}, based on our previous conclusions that B_{vern} depends primarily on river discharge and incident solar radiation (Jassby 2005). The same approach was used as for Equation 1 and Equation 2, resulting in

$$\ln(B_{vern}) = c_1 + c_1 \ln(Q_{sjr}) + c_2 I_0 + \eta_t \quad \textbf{(3)}$$

and

$$(1 - \rho L)(1 - \phi L^{12})\,\eta_t = \varepsilon_t \quad \textbf{(4)}$$

where B_{vern} is Vernalis chlorophyll *a* concentration (µg L^{-1}), Q_{sjr} is San Joaquin River discharge at Vernalis (m^3 s^{-1}), I_0 is incident PAR (mol m^{-2} d^{-1}), and the c_i, ρ, and ϕ are constants. This model required a seasonal autoregressive term instead of a higher-order autoregressive term. The seasonal autoregressive term is at least partly due to, and has the effect of removing, a long-term trend in the relation between phytoplankton biomass and river discharge (Jassby 2005). The coefficient estimates are summarized in Table 5, and the fitted values are plotted in Figure 13.

This model also satisfies all of the criteria described above for Equation 1 and Equation 2. All model parameters are statistically significant. The fitted values correspond well to observed ones (R^2 = 0.71). All autocorrelations and partial autocorrelations are nearly zero at all lags. The Durbin-Watson statistic is 2.0, and Q-statistics are not significant up to at least 12 lags, except for a barely significant value at lag 3 (P = 0.043). The Breusch-Godfrey Lagrange multiplier test indicated no serial correlation up to at least 12 lags (P = 0.11).

We then solved the model in dynamic mode (see Methods) to establish baseline conditions and examine several possible scenarios. Because of uncertainties in model specification, as well as in parameter values, the exact numeric results are of limited value. Rather, the emphasis is on establishing that the three predictors—ammonium load, river phytoplankton biomass, and river discharge—have ecological significance, and not just statistical significance, i.e., that their variability has notable effects on the dissolved oxygen deficit. Scenarios were chosen on the basis of historical distributions of the predictors during June-November.

Table 5. Parameter estimates for model of phytoplankton chlorophyll at the monthly scale. R^2 = 0.71, n = 336 after adjusting endpoints.

Term	*Coefficient*	*Std. Error*	*P*
Intercept	3.6	0.3	<0.001
$\ln(Q_{sjr})$	–0.55	0.05	<0.001
I_0	0.037	0.003	<0.001
ρ	0.25	0.05	<0.001
ϕ	0.27	0.06	<0.001

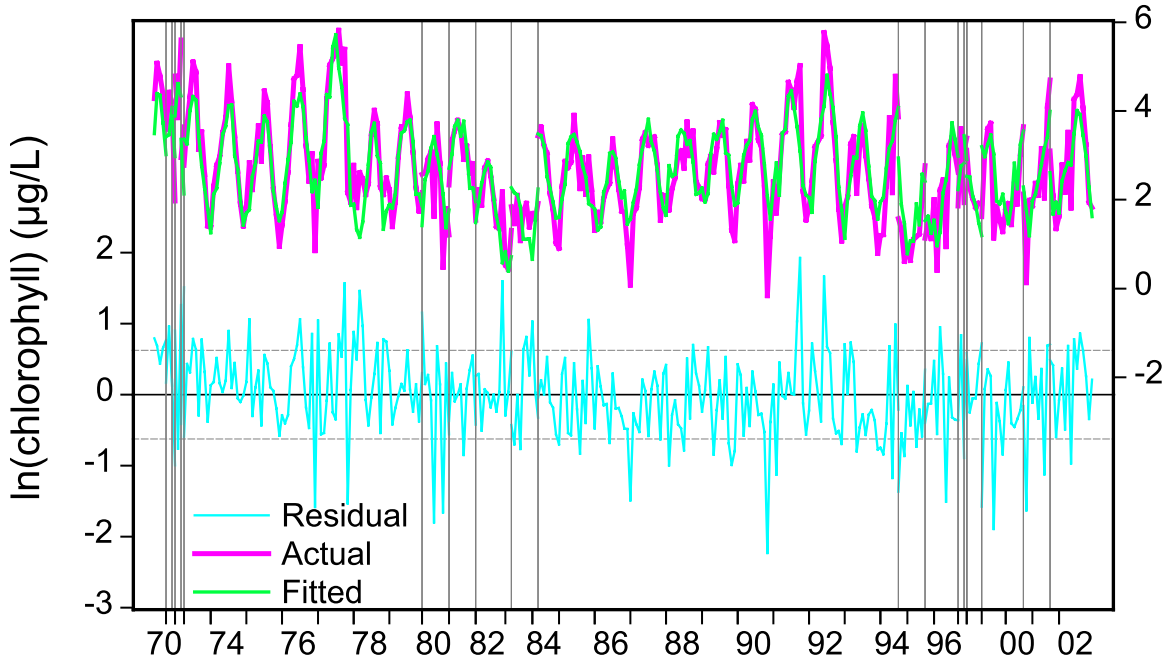

Figure 13. Observations compared with fitted values from the model of Vernalis chlorophyll *a* concentrations (Equations 3 and 4). Vertical lines mark gaps in the monthly data for predictor or response variables.

For L_{amm} and B_{vern}, we examined the effects of maintaining values below, in turn, the following quantiles: 0.1, 0.25, 0.5, 0.75, and 0.9. For example, the 0.25 quantile for ammonium load L_{amm} is 92 kg d^{-1}. In the corresponding scenario, L_{amm} is set equal to observed values for all observations less than 92 kg d^{-1}, but equal to 92 kg d^{-1} for all observations greater than this threshold. The intention is to simulate a management action that would limit actual loading to a maximum of 92 kg d^{-1}. Repeating for each of the five quantiles provides an idea of system response to potential management choices spanning the entire distribution of observed loading values. Because B_{vern} is an endogenous variable of the model, quantiles were based on the baseline solution for B_{vern}, not observed values.

For Q_{sjr}, we examined the effects of maintaining values above, rather than below, these same quantiles. A lower rather than upper limit is used in the case of Q_{sjr}: lower flows increase the incidence of hypoxia and so any management action would involve maintaining actual flows above a certain minimum. To avoid introducing further uncertainties with an additional equation for net discharge, we assumed in the latter scenarios that the barrier at the head of Old River was in place. These scenarios therefore deal with manipulating net discharge through reservoir storage-and-release patterns, but not through water exports or barriers. Results are summarized by the empirical cumulative distribution function for each predictor variable and scenario separately (Figure 14).

The distribution functions illustrate that limiting ammonium loading or phytoplankton carrying capacity would have a similar effect on the dissolved oxygen deficit over the broad range of their historical variability, i.e., from the 0.1 to 0.9 quantile. Specifically, choosing either the 0.75 or 0.9 quantile as an upper limit results in only small changes in the dissolved oxygen distribution compared to baseline conditions. Even the strongest management scenario—namely, choosing the 0.1 quantile as an upper limit—eliminates the dissolved oxygen deficit only about 80% of the time. River discharge has a stronger impact on the dissolved oxygen deficit over its historical range, and the deficit can be eliminated almost completely when discharge is high enough. Moreover, even relatively small constraints on discharge, such as maintaining it above 25 m^3 s^{-1} (the 0.1 quantile), can have a large impact on the dissolved oxygen deficit. Relative to historical variability, then, the dissolved oxygen deficit is most sensitive to river discharge.

Ten additional scenarios were examined for each variable singly and each combination of two or all three. The ten scenarios were obtained by varying the variables from the 0.1 to 0.9 quantile of their historical distribution during June-November by equal numeric intervals (Table 6). Scenario 1 represents the strongest imposition of management actions (i.e., it results in the biggest change from actual historical conditions), whereas Scenario 10 represents the weakest (i.e., most similar to historical conditions). As described above, potential management actions involve setting upper limits for ammonium loading and phytoplankton biomass, but lower limits for river discharge. In quantitative terms, for scenario i, ammonium loading and phytoplankton biomass do not exceed $q_{0.1} + (i-1)(q_{0.9} - q_{0.1})/9$ and river discharge does not drop below $q_{0.9} - (i-1)(q_{0.9} - q_{0.1})/9$, where q_j is the j quantile. Results for each scenario are summarized by a scalar quantity instead of a distribution, namely, the proportion of months in which a dissolved oxygen deficit occurred (Figure 15).

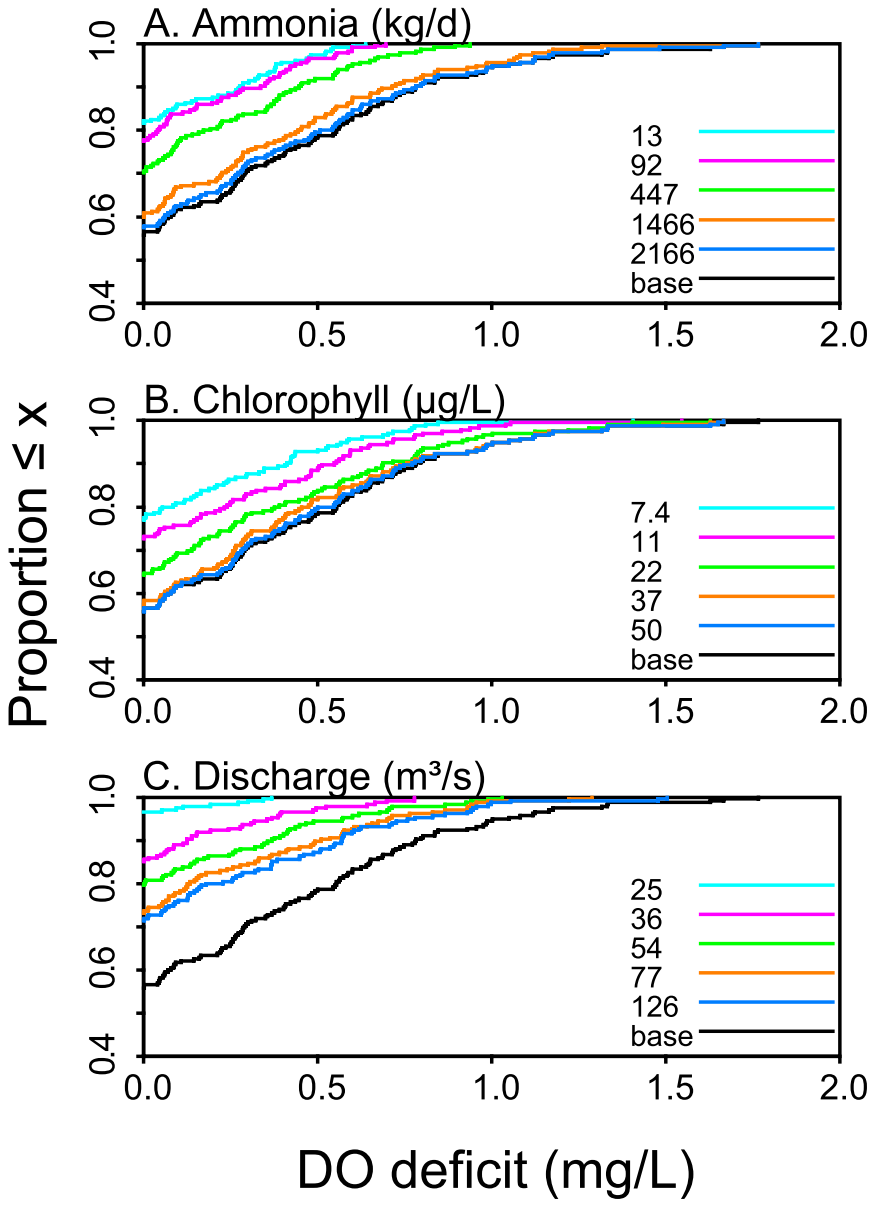

Figure 14. Empirical cumulative distribution functions comparing each scenario to the baseline solution of the model represented by the coupled equations 1-4. Numbers in the key for each plot are the 0.1, 0.25, 0.5, 0.75, and 0.9 quantiles of the historical distributions (June-November). (A) Scenarios in which Wastewater Facility ammonium effluent is maintained below the corresponding quantiles. (B) Scenarios in which the (e.g., nutrient) carrying capacity for chlorophyll at Vernalis is set at the corresponding quantiles. (C) Scenarios in which Vernalis river discharge is maintained above the corresponding quantiles by reservoir releases. For any given deficit on the x-axis, the y-axis shows the proportion of data that have a smaller or equal deficit. The intersections of plot lines with the y-axis therefore show the proportion of data for which there is no deficit.

Table 6. Values used to establish scenarios for impacts on the dissolved oxygen deficit.

Scenario	$max\ L_{amm}$ ($kg\ d^{-1}$)	$max\ B_{vern}$ ($\mu g\ L^{-1}$)	$min\ Q_{sjr}$ ($m^3\ s^{-1}$)
1	13	7.4	126
2	252	12	115
3	491	17	104
4	731	22	92
5	969	26	81
6	1209	31	70
7	1448	36	59
8	1688	41	47
9	1927	45	36
10	2166	50	25

For the scenarios in which one variable was limited (A–C), the patterns reflect the conclusions from the distribution functions. The overall impacts of ammonium loading and phytoplankton chlorophyll are similar. The impact of discharge is largest, and its effectiveness as a management tool (the slope of the curve) remains approximately the same over its historical range. For the scenarios in which two variables were limited (D–F), limiting chlorophyll provides benefits additional to limiting ammonium loading only for strong scenarios. Limiting ammonium or chlorophyll loading—or both (G)—provides benefits additional to managing river discharge, although these are small and almost nonexistent for weak scenarios. The results therefore suggest that relatively weak

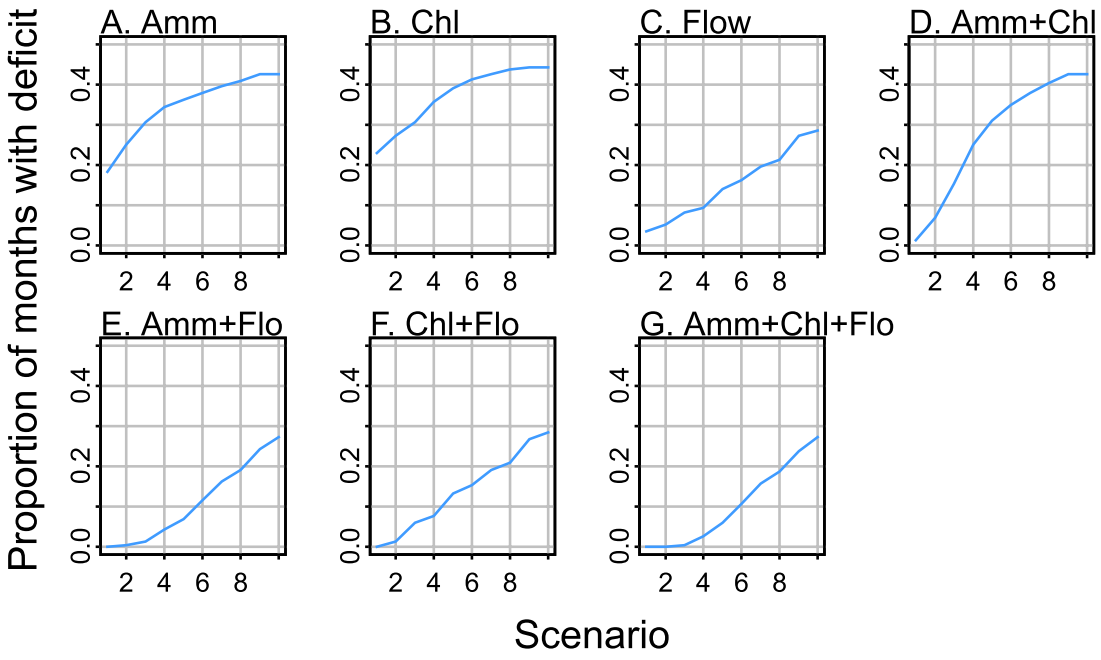

Figure 15. Effects of hypothetical management interventions on dissolved oxygen deficits for the period October 1983 through April 2003. The y-axis represents the proportion of months (with maximum representing 50%) with a deficit. The x-axis represents the 10 scenarios summarized in Table 6. Scenario 1 represents the strongest, and Scenario 10 the weakest, level of management intervention. (A)-(C) Scenarios in which a single predictor changes. (D)-(F) Scenarios in which two predictors change in tandem. (G) Scenarios in which all predictors change in tandem.

management actions could have impacts through river discharge alone, whereas strong actions are required for any scenario that does not involve managing discharge.

A final scenario was examined in which conditions at Vernalis were restored to full natural flow, i.e., flow that would have occurred without any diversion, storage, or water transfers upstream of Vernalis. As illustrated by the seasonal distributions for the simulation period, October 1983 through April 2003, flow management typically causes a decrease in flow during March-July and an increase during September-October (Figure 16). With the barrier at the head of Old River in place, i.e., net discharge into the Ship Channel set equal to discharge at Vernalis, the restoration of full natural flow offers little additional benefit for dissolved oxygen conditions (Figure 17). Although the frequency of intermediate-sized deficits decreases, the frequency of small deficits actually increases. The proportion of months completely free of deficits changes a negligible amount.

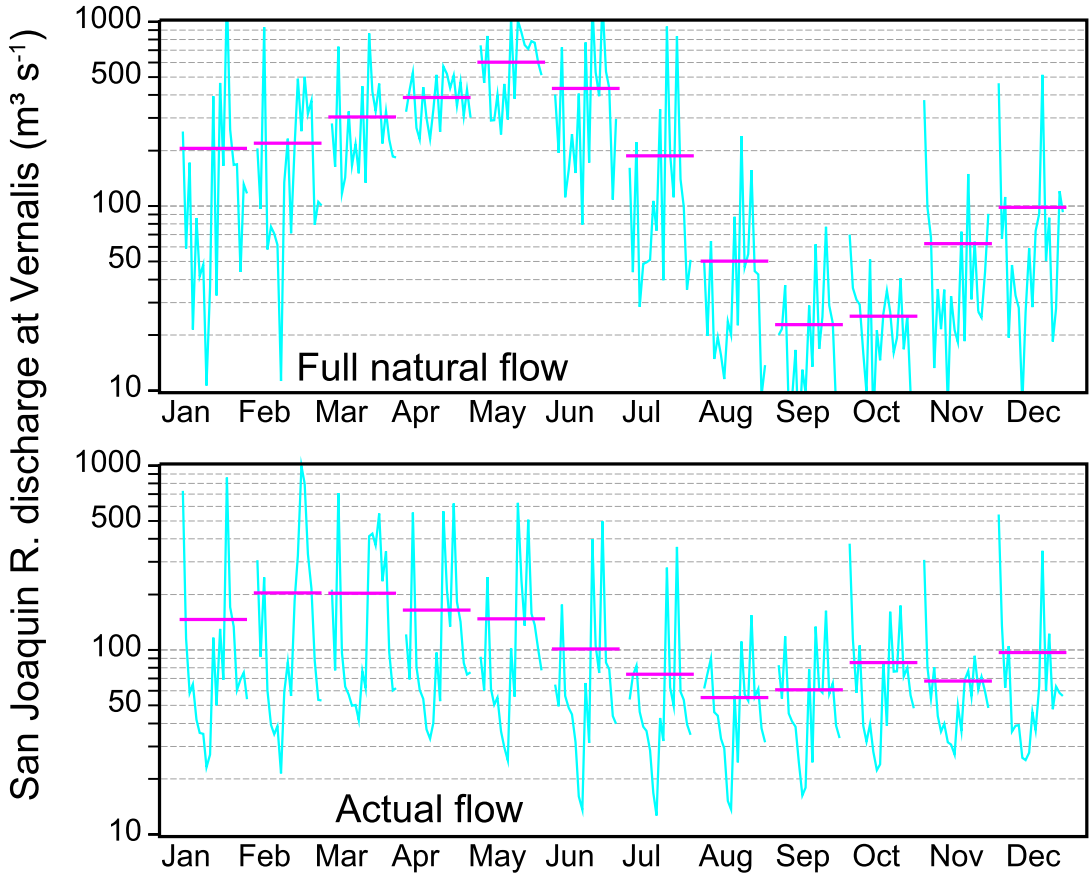

Figure 16. Seasonal distributions of full natural flow and actual flow in the San Joaquin River at Vernalis, October 1983-April 2003. The annual time series for each month is plotted above the month name, and the horizontal line represents the median of the series.

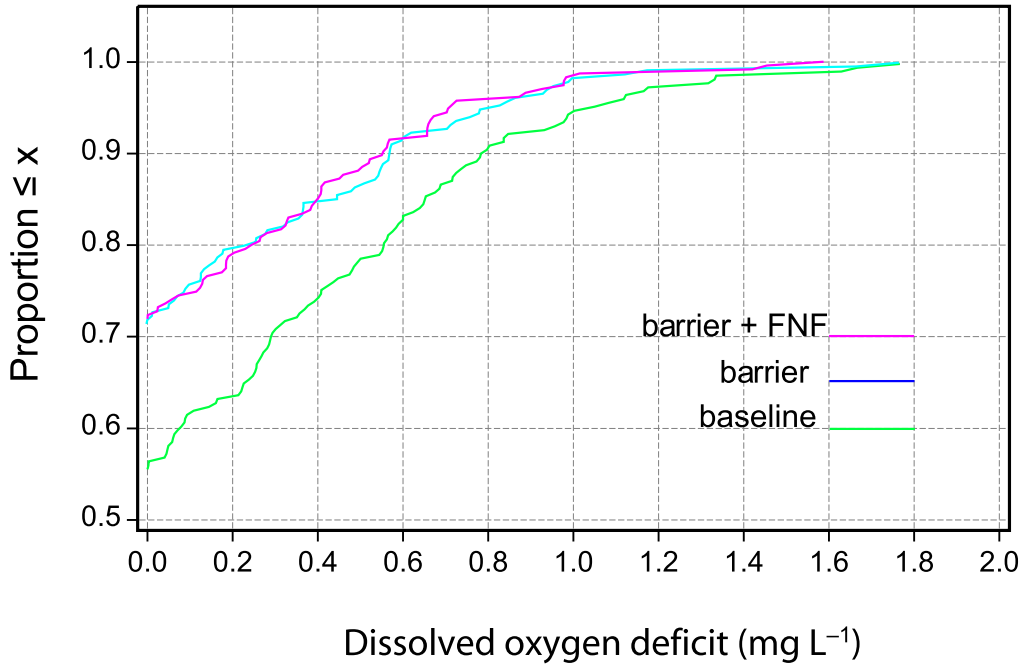

Figure 17. Empirical cumulative distribution functions comparing two scenarios to the baseline solution of the model represented by the coupled equations 1-4. In the barrier scenario, the barrier at the head of Old River remains in place at all times. In the barrier + FNF scenario, flow at Vernalis is additionally set to full natural flow (Figure 16). For any given deficit on the x-axis, the y-axis shows the proportion of data that have a smaller or equal deficit.

DISCUSSION

Causal Factors

The historical database offers a unique opportunity to use statistical methods for determining the important factors underlying hypoxia, or at least the factors responsible for hypoxia variability about the long-term mean for the period of record. The relative importance of different factors can depend on the time scale under consideration. Others have examined the response of dissolved oxygen at the daily to weekly scale (Giovannini and others 2003; Lehman and others 2004). Here, we examined historical variability at the annual and seasonal (monthly) time scales. Our main focus is on those ultimate causative factors that can be managed to some extent, as opposed to factors such as temperature that are proximate causes of dissolved oxygen dynamics but cannot be manipulated practically. In particular, the emphasis is on river discharge, which is controlled by reservoir storage-and-release patterns, as well as water exports via Old River, diversions, and drainage; river phytoplankton biomass, which could be changed by a large reduction in nutrients; and ammonium loading from the Wastewater Facility, which is partly a result of the sewage treatment process.

Although the emphasis for river load is on phytoplankton biomass, other sources of BOD are also present, including particulate and dissolved detritus, as well as ammonium. Because the approach here is based on temporal variability, river phytoplankton is a surrogate for all forms of BOD with which it

covaries. It is probably the dominant particulate form during the severest hypoxic conditions of June-September. Sobczak and others (2002), for example, concluded that phytoplankton constitute essentially all of the bioavailable particulate organic matter in the Delta, including the San Joaquin River (Mossdale sampling station). Their findings were based on a series of bioassays conducted over two years under varying hydrographic conditions and seasons. In particular, the estimated mean phytoplankton carbon was always at least 100% of the estimated bioavailable particulate organic carbon, and the two were also highly correlated. Their results are consistent with a recent study by Kratzer and others (2004) based on data collected in 2000 and 2001. These researchers concluded on the basis of carbon-to-nitrogen ratios and the δ^{13}C of particulate organic matter in the San Joaquin River that it was comprised primarily of phytoplankton during June-September. In contrast, dissolved BOD does appear to be significant. We estimated that phytoplankton accounted for only 34% of ultimate BOD during June-September 2001 at Mossdale, based on the data synthesized by Lee and Jones-Lee (2002, Table D-3). Even including phytodetritus based on pheophytin concentrations, the ratio rises to only 60%. Ammonium accounts for 20% and presumably dissolved organic matter the remaining 20%. The latter two could be in part extracellular and degradation products of phytoplankton and phytodetritus, but probably originate directly from agricultural sources, including animal wastes (Kratzer and Shelton 1998; Kratzer and others 2004). Insofar as these other sources do not covary with phytoplankton, they are a source of uncertainty in the analyses and models of this study. The historical record is inadequate to address this uncertainty: long-term measurements include only dissolved ammonium, not ammonium attached to particles, and the BOD equivalence of dissolved detritus is also highly uncertain.

In a similar fashion, ammonium is used as a surrogate for BOD in Wastewater Facility effluent. Ammonium is the only effluent measurement that provides a sufficiently long record. Five-day total BOD values are available, but samples have a high total kjeldahl nitrogen relative to their organic carbon content, which could render these BOD tests carbon-limited and the results too low. Overall, ammonium accounted for a median of 63% of the Wastewater Facility BOD load during 1981-2003. In some months, however, especially June and July, the contribution is much smaller. Moreover, the correlations between ammonium and the other main BOD fractions in the effluent, carbonaceous BOD and total organic nitrogen, are statistically significant but relatively small (0.14 and 0.39, respectively). As in the case of river phytoplankton, then, the use of ammonium as a surrogate for wastewater BOD is a potentially important source of uncertainty in the analyses and models here.

Despite the uncertainty, the annualized data imply significant roles for river phytoplankton and wastewater effluent (Figure 10). With regard to river discharge, we can say only that the annual data are inconclusive. As the monthly data show, this is a consequence of the time scale of analysis. In fact, even at the annual scale, it is possible to show the influence of river discharge over other averaging periods. A proper analysis must include all three variables simultaneously. Simulation studies suggest, however, that 10 to 20 observations per parameter, apart from the intercept, is a desirable goal in multivariate regression (Harrell and others 1996). The ability to account for more than two predictor variables is therefore very limited with only 19 annualized observations. The only way to distinguish among these factors with the

current data set is to examine them at a shorter time scale. The real value of the annualized data is to provide striking evidence for the role of Wastewater Facility ammonium loading. The close correspondence between minimum dissolved oxygen and ammonium loading was unexpected, and it confirms at a different time scale the case made by Lehman and others (2004) for the importance of nitrogenous BOD in the Ship Channel.

Indeed, the importance of all three factors is revealed clearly at the monthly scale by the comparison of above-median versus below-median data (Figure 11). The confidence intervals for these boxplot medians are underestimates, as they assume independence among data, which may not be strictly true for months in the same year. Nonetheless, the differences in medians are striking. No observations exist for cases F and H simply because high river discharge lowers the residence time for phytoplankton and prevents the development of high phytoplankton concentrations. This part of the retrospective analysis, in particular, is a direct demonstration of the role of nonpoint river loads, which does not emerge from the annualized data. River loads have been identified as the dominant BOD load based on a small set of years (1999-2001; Lee and Jones-Lee 2002; Lehman and others 2004). The Environmental Monitoring Program historical data set, unfortunately, does not include regular BOD measurements. In theory, one could use the nitrogenous BOD equivalent of total kjeldahl nitrogen and the carbonaceous BOD equivalents of dissolved and particulate organic carbon measurements from this program, but the uncertainty in these BOD equivalent values is high. The retrospective statistical evidence is therefore welcome additional evidence for the sustained long-term importance of river loads.

The time-series regression model also supports a role for each of the three predictor variables (plus two others) at the monthly scale (Table 4). Note that each term has a sign consistent with the most likely causal mechanism. An increase in net discharge should increase dissolved oxygen, whereas an increase in the supply of river phytoplankton or wastewater ammonium loading should decrease it. Higher temperatures, by favoring both decomposition and nitrification, should also decrease dissolved oxygen. To understand the positive effect of channel phytoplankton, recall that the discrete water quality sampling is located near the water surface. The net effect of phytoplankton in the upper layers is to increase dissolved oxygen through net positive photosynthesis. If the monitoring and sampling were located near the bottom, an opposite sign would be expected. Although all terms are statistically significant, the standard errors suggest that the role for channel phytoplankton is weakly established by this analysis compared to other predictors. Even so, the standard errors are highly dependent on the exact equation specification, which is constrained in turn by data availability, and so the relative errors are of limited value in establishing ecological importance. For example, because the amount of net growth occurring between Vernalis and the Ship Channel depends on Q_{net}, phytoplankton concentration entering the Ship Channel also depends on Q_{net}. Consequently—were sufficient data available—loading should be specified as a more complex function of B_{vern} and Q_{net} than the term $a_2 \ln(B_{vern}) \ln(Q_{net})$ in Equation 1.

Management Scenarios

There are two major challenges in time-series regression models: specifying the exact way that the predictor variables enter into the equation, and determining the model for the residual terms. In principle, the equation specification should reflect the underlying

mechanisms. In a data-based model, however, reliable parameter estimation depends on the ratio of parameters to observations, which can severely limit the form of the equation. As the specification becomes a more detailed and more accurate description of underlying mechanisms, the number of parameters increases. If there are too many parameters to estimate for the amount of available data, however, the forecasting capability of the model will be exaggerated. In particular, R^2 will not be a good guide to the difference between predicted and actual future values, a problem known as *overfitting* (Harrell 2001). Ecological time series are typically long enough to allow accurate description of the underlying causes only for very simple mechanisms (e.g., Jassby and others 2003). Although there are about 20 years of monthly observations available for analysis here (after data imputation), the serial correlation introduced by seasonality implies a much smaller number of effective observations. Recall that at least 10 and preferably 20 observations per variable should be used in a multivariate regression. We therefore believe that the model specification must be kept as simple as possible to minimize the number of parameters to be estimated, considering the number of predictor variables and the additional need to model the residuals. We have tried to incorporate in Equations 1-4 the minimum set of variables and the simplest description of processes that reflect current understanding and data availability.

The forecasting scenarios are best interpreted qualitatively and relatively. In regression models, the calibration curve—the plot of predicted versus observed behavior—is always biased. Predicted extreme values tend to be biased toward the mean, resulting in a calibration slope less than one, a phenomenon known as shrinkage (Harrell 2001). This is manifested in the distribution for the baseline solution, which shows a maximum deficit of less than 2 mg L^{-1}. In fact, there were a total of 8 (out of 202) months in which the deficit exceeded 2 mg L^{-1}. Accordingly, the scenarios must be compared to the baseline solution and not the original data, and emphasis needs to be on relative rather than numerical results. Recall also that the data represent near-surface values, not the depths of most intense hypoxia. Even if shrinkage did not occur, the relative results would therefore still be of most interest.

The scenarios suggest that, relative to their historical range, wastewater loading and nonpoint river sources have a similar impact on hypoxia, with wastewater loads exerting a somewhat stronger influence (Figure 14 and Figure 15). The scenarios are therefore consistent with the direct comparison of data binned with respect to their medians (Figure 11, comparing A to C and A to E). The dissolved oxygen sources and sinks data, synthesized by Lee and Jones-Lee (2002) in terms of a box model, imply that nonpoint river oxygen demand actually exceeds point-source wastewater oxygen demand by a factor of over three. One would therefore expect that a decrease in maximum wastewater loads would have a smaller impact than an equivalent decrease in phytoplankton carrying capacity, whereas our model suggests that the impacts are similar. There are several possible reasons for this discrepancy. A prominent one is that the box model is based on a specific set of flow conditions, whereas the analysis presented here represents behavior over a period of 20 years with widely varying flow conditions. Also, as emphasized by Lehman and others (2004), it is necessary to account for different oxidation rates in comparing the impact of wastewater treatment plant versus upstream nonpoint organic loads. Still, it should be said that the box model is based on measurement of all wastewater BOD components and actual river BOD, however limited in duration, whereas this analysis uses wastewater ammonium and phytoplankton chlorophyll *a* as indices of BOD,

and near-surface dissolved oxygen as an index of hypoxia. Perhaps most important is that these completely independent approaches concur on both sources being of importance and (very) approximately the same magnitude; the scenarios can be seen as generalizing the box model conclusions to the range of historical conditions.

The scenarios also imply that control of either river load or Wastewater Facility load alone is insufficient to eliminate hypoxia (Figure 15). In the case of river phytoplankton, reduction of nutrients to limit phytoplankton carrying capacity below 25 μg L^{-1} chlorophyll *a*—sometimes considered the threshold between mesotrophic and eutrophic conditions (OECD 1982), and essentially the same as the median scenario in Figure 14—would still leave deficits more than one-third the time. This is consistent with the direct analysis of the binned data in which dissolved oxygen is strongly depressed when either factor is elevated, even if the other is lower than normal. Given that near-surface dissolved oxygen provides a low estimate of hypoxic conditions, however, elimination of either in reality must leave an even larger proportion of months with a deficit than suggested by these plots. It is gratifying that eliminating both sources simultaneously does virtually eliminate the deficit, because it reflects an internal consistency in the model that is a consequence not merely of the way in which it was specified but also of the parameter estimates based on historical data. Because river phytoplankton and wastewater ammonium loading are both surrogates, we must be cautious about identifying nonpoint source management with phytoplankton control, and point source management with ammonium control. Especially in the case of wastewater, elimination of ammonium alone through enhanced nitrification will still leave a large BOD load, historically (1981–2003) approximately half the total during June–November. Similarly, reduction of river phytoplankton could still leave a large dissolved detritus and total ammonium load originating in agricultural and animal sources upstream. For example, phytoplankton populations in the river near Vernalis have become increasing phosphorus-limited (Jassby 2005). Reducing phosphorus alone could reduce the carrying capacity for phytoplankton and phytoplankton-associated BOD load, but leave other important sources unchanged. In recent years, the ratio of dissolved to particulate organic carbon loads at Vernalis has ranged from about four during peak phytoplankton season to about nine during the winter (Saleh 2003); even given the typical low bioavailability of dissolved detritus in the Delta (Sobczak 2002), the potential exists for an important contribution by non-phytoplankton organic matter. The emphasis therefore has to be on management of the broad spectrum of both wastewater and nonpoint river loads. As discussed by Jassby (2005), a slight complication is introduced by the fact that phytoplankton growth rate is light-limited in the San Joaquin River. If mineral suspensoid loads are reduced along with nutrient and organic matter loads, the increase in growth rate could lead to higher phytoplankton loads unless the nutrient-associated carrying capacity is reduced sufficiently.

River discharge has had the biggest impact of all on hypoxia over the historical range of variables (Figure 15). Even the weakest river management scenario results in substantial decreases in the proportion of months with hypoxia. The strongest eliminates most of the near-surface deficits on its own; in combination with wastewater or nonpoint river management, the elimination is complete. Of course, the river discharge scenarios also assume that the barrier at the head of Old River is in place, which alone produces substantial relief from hypoxic conditions (Figure 17), a decrease in the proportion of

months with deficits from 0.44 to 0.28. In fact, the weakest of river discharge scenarios can be seen as primarily representing the effect of the barrier. But river discharge has strong additional effects as well, as shown by the magnitude of change over the remainder of the scenarios (Figure 15). One reason discharge has such large effects is that—as pointed out above and expressed in Equation 3—higher discharge reduces river phytoplankton concentration (as well as the concentration of other nonpoint BOD sources in the river such as ammonium, although the connection is looser), in addition to its direct effects on dissolved oxygen balance in the Ship Channel. Consequently, higher discharge does not simply export the hypoxia problem downstream: not only is the concentration of BOD sources lower, but downstream channel geometry is not as conducive to hypoxia.

It may seem that management of river discharge offers an effective tool, immediately at hand, for addressing the hypoxia problem, one that could produce effects with only weak management actions. The choice of which combination of variables to manage, and to what level, is an optimization problem that obviously involves more dimensions than the single one addressed here. One dimension could be described as responsibility. We defined weak and strong scenarios in relation to historical variability, not in relation to any absolute values, and without regard to the fact that some of the historical values are extreme in a broader context. For example, phytoplankton concentrations reaching well above 100 μg L^{-1}, and occasionally above 300 μg L^{-1}, reflect hypereutrophic nutrient concentrations from anthropogenic nonpoint sources. It is probable that background nutrient concentrations would maintain phytoplankton at much lower levels, sufficient to have an effect on the dissolved oxygen deficit, regardless of flow impairment. The fact that these levels now require a strong management action reflects the extent to which nonpoint pollution has been allowed to proceed in the watershed, and cannot be used as justification for ignoring it. This pertains even more so for Wastewater Facility effluent, which has a zero background load but which has been increasing at an average rate of over 10% per year since 1982.

Ironically, changes in upstream storage-and-release patterns from years before construction of the Central Valley Project appear to be approximately neutral with respect to hypoxic conditions. Discharge at Vernalis is generally lower than unimpaired runoff, or full natural flow, in the San Joaquin River during spring and early summer, and higher during late summer and autumn (Figure 16). Highest river phytoplankton concentrations are usually attained in July, toward the end of the period when managed flow is less than full natural flow. Current flow management therefore probably exacerbates conditions through midsummer. Although managed flow is typically higher than full natural flow after the phytoplankton peak, the net effect on the Ship Channel compared to unmanaged flow is not *a priori* positive during this later period. Recall that the model for dissolved oxygen contains lags of up to two months, representing the memory of loading in the recent past, which at least in principle could overwhelm any positive increment in current discharge. The scenario in which river discharge is restored to full natural flow resolves this question: the trade-off between early and late summer is reversed, but the net effect on frequency of hypoxia remains about the same. The barrier at the head of Old River appears to have much more importance for historical dissolved oxygen conditions than the difference between unimpaired and actual flows upstream of Old River. Its role at the monthly scale here is consistent with strong effects reported for shorter time scales (Giovannini and others 2003). Unfortunately,

the methods used here do not allow us to compare unimpaired with actual flows when the barrier is not in place and water is exported down Old River.

The low dissolved oxygen conditions in the Ship Channel are far from unique. Hypoxic conditions are common in estuaries, including their tidal river subregions. The most common reason is nitrogen overenrichment and subsequent organic matter production in the form of phytoplankton (NRC 2000). Bricker and others (1999) identified 44 highly enriched estuaries in the United States alone, with an additional 36 moderately enriched estuaries. The most important nitrogen sources are nonpoint, including agriculture and deposition of fossil fuel combustion products. Nitrogen from animal wastes leaking directly to surface waters or first volatilizing as ammonia is often the largest single source for estuaries. The San Joaquin River watershed is no different in this respect, with much if not most of the nitrogen originating as animal waste (Kratzer and Shelton 1998; Kratzer and others 2004). The complexity of controlling mechanisms, though, which it shares with other dredged river channels receiving agricultural and wastewater inputs, has stimulated a large amount of diverse monitoring, experimentation, and modeling. Here, we have tried to add a new perspective to these studies through analysis of the comprehensive long-term data. These data help to delineate more precisely the role of river phytoplankton, Wastewater Facility effluent, the seasonal pattern and amount of river discharge, and state of the Old River barrier—all under human influence—in determining dissolved oxygen conditions in the Ship Channel.

Acknowledgments

We gratefully acknowledge support for this research from the California Bay-Delta Authority (ERP-02-P33 and contract 4600001642). We also thank three anonymous reviewers for their helpful comments, and Larry Huber and Peggy Lehman for information on Wastewater Facility effluent.

References

Bain RC, Pierce WH, Kato A. 1968. An analysis of the dissolved oxygen regimen in the San Joaquin Estuary near Stockton, California. San Francisco (CA): U.S. Dept. of the Interior, Federal Water Pollution Control Administration, Southwest Region.

Bricker SB, Clement CG, Pirhalla DE, Orlando SP, Farrow DRG. 1999. National Estuarine Eutrophication Assessment: Effects of nutrient enrichment in the nation's estuaries. Silver Spring (MD): U.S. Dept. of Commerce, National Oceanic and Atmospheric Administration.

[CDWR] California Dept. of Water Resources. 2004a. California Data Exchange Center. Sacramento (CA): California Dept. of Water Resources. Available at: http://cdec.water.ca.gov. [Accessed 24 August 2004.]

[CDWR] California Dept. of Water Resources. 2004b. California Irrigation Management Information System. Sacramento (CA): California Dept. of Water Resources. Available at: http://www.cimis.water.ca.gov. [Accessed 23 January 2004.]

Chapra SC. 1997. Surface water-quality modeling. New York: McGraw-Hill.

Cloern JE, Grenz C, Vidergar-Lucas L. 1995. An empirical model of the phytoplankton chlorophyll:carbon ratio-the conversion factor between productivity and growth rate. Limnology and Oceanography 40:1313-1321.

[CVRWQCB] Central Valley Regional Water Quality Control Board. 1998. The water quality control plan (Basin Plan) for the California Regional Water Quality Control Board Central Valley Region. 4th ed. The Sacramento River Basin and the San Joaquin River Basin. Sacramento (CA): Central Valley Regional Water Quality Control Board.

[CVRWQCB] Central Valley Regional Water Quality Control Board. 2003. Total Maximum Daily Load for low dissolved oxygen in the San Joaquin River. Sacramento (CA): Central Valley Regional Water Quality Control Board.

Giovannini P, Giulianotti JC, Hayes SP. 2003. Dissolved oxygen and flow in the Stockton Ship Channel, fall 2002. IEP Newsletter 16:30-34. Available at: http://iep.water.ca.gov/report/newsletter/

Gowdy M, Foe C. 2002. San Joaquin River low dissolved oxygen Total Maximum Daily Load: interim performance goal and final target analysis report. 25 Apr 2002 draft. Sacramento (CA): Central Valley Regional Water Quality Control Board.

Gómez V, Maravall A. 2002. Seasonal adjustment and signal extraction in economic time series. Chapter 8. In: Pena D, Tiao GC, Tsay RS, editors. A course in time series analysis. New York: Wiley.

Hallock RJ, Eldwell RF, Fry DH. 1970. Migration of adult king salmon *Oncorhynchus tshawytscha* in the San Joaquin Delta, as demonstrated by the use of sonic tags. Fish Bulletin 151. Sacramento (CA): California Dept. Fish and Game.

Harrell FE Jr, Lee KL, Mark DB. 1996. Multivariable prognostic models: issues in developing models, evaluating assumptions and adequacy, and measuring and reducing errors. Statistics in Medicine 15:361-387.

Harrell FE Jr. 2001. Regression modeling strategies: with applications to linear models, logistic regression, and survival analysis. New York: Springer.

Harvey AC. 1993. Time series models, 2nd ed. Cambridge (MA): MIT Press.

[IEP] Interagency Ecological Program for the San Francisco Estuary. 2003. Dayflow. Sacramento (CA): Interagency Ecological Program for the San Francisco Estuary. Available at: http://iep.water.ca.gov/dayflow. [Accessed 2 May 2003.]

Jassby AD, Reuter JE, Goldman CR. 2003. Determining long-term water quality change in the presence of climate variability: Lake Tahoe (USA). Canadian Journal of Fisheries and Aquatic Sciences 60:1452-1461.

Jassby AD. 2005. Phytoplankton regulation in a eutrophic tidal river (San Joaquin River, California). San Francisco Estuary and Watershed Science [online]. Vol. 3, Issue 1 (March 2005), Article 3. Avaliable at: http://www.estuaryscience.org/vol3/iss1/art3/.

Kratzer CR, Shelton JL. 1998. Water quality assessment of the San Joaquin-Tulare basins, California: analysis of available data on nutrients and suspended sediment in surface water, 1972-1990. Professional Paper 1587. Denver (CO): U.S. Geological Survey.

Kratzer CR, Dileanis PD, Zamora C, Silva SR, Kendall C, Bergamaschi BA, Dahlgren RA. 2004. Sources and transport of nutrients, organic carbon, and chlorophyll-*a* in the San Joaquin river upstream of Vernalis, California, during summer and fall, 2000 and 2001. Water-Resources Investigations Report 03-4127. Sacramento (CA): U.S. Geological Survey.

Lee GF, Jones-Lee A. 2002. Synthesis of findings on the causes and factors influencing low DO in the San Joaquin River Deep Water Ship Channel near Stockton, CA. Report submitted to the SJR DO TMDL Steering Committee/Technical Advisory Committee and CALFED Bay-Delta Program. El Macero (CA): G. Fred Lee & Associates.

Lehman PW, Sevier J, Giulianotti J, Johnson M. 2004. Sources of oxygen demand in the lower San Joaquin River, California. Estuaries 27:405-418.

Morel A, Smith RC. 1974. Relation between total quanta and total energy for aquatic photosynthesis. Limnology and Oceanography 19:591-600.

[NRC] National Research Council. 2000. Clean coastal waters: understanding and reducing the effects of nutrient pollution. Washington, D.C.: National Academy Press.

Newey W, West K. 1987. A simple positive semi-definite, heteroskedasticity and autocorrelation consistent covariance matrix. Econometrica 55:703-708.

[OECD] Organization for Economic Cooperation and Development. 1982. Eutrophication of waters. Monitoring, assessment, and control. Final report. Paris: Organization for Economic Cooperation and Development, Environment Directorate, Cooperative Programme on Monitoring of Inland Waters (Eutrophication Control).

Saleh DK, Domagalski JL, Kratzer CR, Knifong DL. 2003. Organic carbon trends, loads, and yields to the Sacramento-San Joaquin Delta, California, water years 1980-2000. Water-Resources Investigations Report 03-4070. Sacramento (CA): U.S. Geological Survey.

Sobczak WV, Cloern JE, Jassby AD, Müller-Solger AB. 2002. Bioavailability of organic matter in a highly disturbed estuary: the role of detrital and algal resources. Proceedings of the National Academy of Sciences 99:8101-8105.